2-7-2008

Modeling the effects of proton irradiation [on] CIGS solar cells

Jacob Dunken

Jacob L. Dunken
Candidate

Electrical and Computer Engineering
Department

This thesis is approved, and it is acceptable in quality
and form for publication on microfilm:

Approved by the Thesis Committee:

_____ , Chairperson

_____

_____

_____

_____

_____

Accepted:

_____
Dean, Graduate School

_____
Date

MODELING THE EFFECTS OF PROTON IRRADIATION

CIGS SOLAR CELLS

BY

JACOB L. DUNKEN

B.S., Electrical Engineering, New Mexico
Institute of Mining and Technology, 2000

THESIS

Submitted in Partial Fulfillment of the
Requirements for the Degree of

Master of Science
Electrical Engineering

The University of New Mexico
Albuquerque, New Mexico

December, 2007

DEDICATION

This is dedicated to my parents Judy and Lee who have encouraged and stood behind me for these many years. This would not be possible without your ongoing support and aid.

Near the completion of this project, my father, Lee, passed away. I hope he knows how much he has encouraged and supported me all of these years and that he is deeply missed and loved greatly. Words alone cannot do him justice.

ACKNOWLEDGMENTS

I would like to thank my advisor, Dr. Charles Fleddermann, for his support throughout this project. This project would not have been possible without his guidance and aid.

I would also like to thank Dr. Jennifer Granata for all of her help with this project. She has provided data, information, and guidance that was invaluable in completing this project.

I would also like to thank Dr. Jingkuang Chen for agreeing to be part of my thesis committee.

MODELING THE EFFECTS OF PROTON IRRADIATION

CIGS SOLAR CELLS

BY

JACOB L. DUNKEN

ABSTRACT OF THESIS

Submitted in Partial Fulfillment of the
Requirements for the Degree of

**Master of Science
Electrical Engineering**

The University of New Mexico
Albuquerque, New Mexico

December, 2007

MODELING THE EFFECTS OF PROTON IRRADIATION

CIGS SOLAR CELLS

BY

JACOB L. DUNKEN

B.S., Electrical Engineering, New Mexico Institute of Mining and Technology, 2000
M.S., Electrical Engineering, The University of New Mexico, 2007

ABSTRACT

The space environment is very harsh on photovoltaic devices. Solar protons (hydrogen ions) cause large numbers of vacancies, which act as recombination centers at deep levels and can create compensating defects that reduce the acceptor concentration at shallow levels in semiconductors. This in turn, can reduce the output power generated by photovoltaic devices. Damage can also occur from atomic oxygen, plasma discharges and electron irradiation.

Solar arrays have to be manufactured to produce more power than necessary so that the solar array will still produce the needed amount of power after degradation occurring from charged particle irradiation. A major challenge is to be able to model these devices so that the effects of charged particle irradiation can be taken into account in calculations for the End of Life (EOL) open-circuit voltage, short-circuit-current, fill-factor, and efficiency. Models presently being used do not provide distinct values without more calculations. Also, models presently being used tend to have proton

irradiation incident normal to the surface, which does not reflect actual conditions, and require a significant amount of input data.

In an effort to correct these problems, a new model was created that finds the remaining factor of the normalized basic cell parameters for $CuInGaSe_2$ (CIGS) solar cells. This model uses significantly fewer inputs than other computer models, provides a more realistic model with respect to entry angles of incident protons, and provides actual and normalized values without extra calculations.

TABLE OF CONTENTS

LIST OF FIGURES

LIST OF TABLES

CHAPTER 1 INTRODUCTION

1.1   Background

Solar photovoltaics is becoming an enticing technology for power production as domestic power prices increase, supplies of traditional fuels decrease, and as concerns about global warming increase.

For terrestrial applications, there are many choices of solar cells available. In the following, a small sampling, by no means an exhaustive list, of what is available for terrestrial use is presented. All devices discussed were tested under Standard Test Conditions (STC) using an Air Mass 1.5 (AM1.5) spectrum. Air mass can be defined as the amount of attenuation of the solar light spectrum [1], [2]. AM1 is defined as the solar spectrum through the atmosphere if the sun is located directly above the solar cell being tested, whereas higher air mass values are generated if the sun is located at a different angle to the solar cell [2]. AM0 is the solar spectrum in space and is used for testing solar cells that are to be deployed in space such as on satellites [1], [3]. BP Solar produces silicon nitride single crystal and multi-crystalline solar cells [4], [5]. Though no information was given on the individual cells, the 175 W solar modules have short-circuit currents of 5.4 A, and open-circuit voltages of approximately 44.0 V [4], [5]. Sharp produces a poly-crystalline solar cell with a module efficiency of 12.8 % [6]. Global Solar produces flexible $CuInGaSe_2$ (CIGS) solar cells which allow for the solar module to be moved easily so that it can be used for many applications [7], [8]. Again, no information was provided on the actual solar cell, but the 25 W module has an open-circuit voltage of 25 V and a short-circuit current of 2.1 A [7], [8].

Solar power in space has been used for several decades aboard satellites [9]. Presently there are two main types of solar cells used in space. The first is traditional silicon cells where the best efficiency in production is 18% at AM0 [10]. Presently the highest efficiency solar cells are multi-junction III-V cells (GaInP/GaAs/Ge) which have an efficiency under an AM0 spectrum of over 30%, and 28% in production [9], [11]. Multi-junction cells made from III-V materials are also being made on flexible substrates and have obtained efficiencies near 30% under an AM0 spectrum [11].

Flexible and lightweight solar cells are being developed so more solar cells and thus more power generation capability can be carried on a satellite in a smaller area [12]. One material being used is $CuInGaSe_2$ (CIGS) which is of interest for several reasons. First, it is light-weight compared to traditional silicon and gallium arsenide cells. This has the potential to lower the cost of launching satellites into orbit which are approximately $22,000/kg for a satellite going into geosynchronous orbit and $10,000/kg for a low Earth orbit [9]. It also has the potential to be manufactured at a much lower cost than crystalline solar cells [9]. In addition, radiation damage can be annealed out of the CIGS material lengthening the life of the cell [13]. One issue with CIGS solar cells is that they have a lower efficiency than GaAs solar cells [9], [14]. CIGS has the potential to reach efficiencies on par with crystalline silicon in production, but as yet that has not been achieved [10], [14], [15], [16].

One of the biggest concerns with solar cells in space is the degradation of the cell by means of charged particle irradiation [17]. In this project, the effects of solar protons (hydrogen ions) will be studied to determine their impact on the basic cell parameters: open-circuit voltage (V_{oc}), short-circuit current (I_{sc}), fill-factor (FF), and efficiency (η).

1.2   The Space Environment

In order to understand space solar cell performance in space applications, it is important to understand the space environment where the cells are used. The three orbits in which most satellites and other space vehicles orbit, are: Low Earth orbit (LEO) [18], Medium Earth Orbit (MEO) [19], and Geosynchronous Earth Orbit (GEO) [20]. LEO, is an orbit that is defined as being at an altitude between 200 and 2000 km above the surface of the Earth [18]. An MEO orbit is defined as being at an altitude between 2000 and 35,786 km [19]. Although there are different types of GEO, the basic idea is that the time the satellite takes to rotate around the Earth is the same time that it takes for the Earth to rotate around its axis one time [20]. One type of GEO orbit is a geostationary orbit over the equator and is at an altitude of 35,786 km above the surface of the Earth [20].

At each orbit, there are charged particles such as protons and electrons as well as heavy ions such as oxygen [12], [21]. Quantities of charged particles vary depending on the orbit [22]. In general, electron fluences are the highest at GEO and are the lowest at a LEO [22]. Proton fluences are the highest at MEO [22]. The next highest fluences of protons occur at a GEO and then at a LEO [22].

1.3   Basic Material Properties

CIGS based solar cells have a direct band-gap which can be between about 1.0 eV and 1.7eV and is determined by the amount of gallium in the material [1], [2], [15]. Unlike silicon which has a tetrahedral lattice, CIGS material has a chalcopyrite lattice [1]. The absorption coefficient is related to the band-gap energy of the material [2]. As the band-gap energy changes with composition, a precise value cannot be given without

knowledge of the band-gap energy, though in general the absorption coefficient is above

10^5 cm^{-1} for wavelengths up to approximately 0.8 μm [23], [24]. Other parameters

include the density of states in the conduction and valence bands which are 2.2x10^{18} cm^{-3}

and 1.8x10^{19} cm^{-3}, respectively [25]. The electron mobility has been documented by

Gloeckler et al. [25] as 100 cm^2/Vs and the hole mobility as 25 cm^2/Vs as compared to

Rockett [26] who documented the electron mobility as 8 cm^2/Vs and the hole mobility as

8 cm^2/Vs. It should be noted that the electrical properties discussed change with growth

parameters and material quality [15]. The values used in simulations in this project are

idealized values.

1.4   Cell Design

In the following sections, different aspects of the design and manufacture of CIGS

solar cells will be discussed.

1.4.1   Effects of Composition

The composition and addition of different elements have great effects on the

properties of the absorber material and the overall cell. In the following, the effects of

gallium and sodium will be examined.

Gallium, in the proper amounts, allows for the manufacture of some of the best

CIGS solar cells known [15]. Cells with an efficiency of 17.7% have been produced

when the ratio of Ga to the sum of Ga + In is in the range of 0.1 to 0.3 [15]. It should be

noted that the test conditions producing the aforementioned 17.7 % efficiency were not

given [15]. When the ratio exceeds this range, the efficiency of the cell degrades and

recombination rates increase due to tunneling [15]. Tunneling is caused by an excessive

doping concentration, causing the short-circuit current to decrease and limiting the open-

circuit voltage [1], [2], [15]. Thin film materials containing Ga have a higher

conductivity due to an increased carrier density [15].

One way to significantly improve the open-circuit voltage and efficiency of CIGS

based solar cells is to add sodium (Na) [27]. Sodium present in concentrations of

approximately 10^{20} cm^{-3} has the effect of increasing the doping level by roughly 10^{16} cm^{-3}

[15]. One theory discussed by Rau and Schock [15] is that the Na atoms take the place of

In or Ga atoms within the lattice and act as a dopant [15]. Rudmann et al. [28], though

not discounting the theory just mentioned, propose that the Na passivates grain

boundaries which reduces recombination and increases the performance of the solar cell.

Another theory discussed by Rau and Schock [15] is that the difference between the

amount of Na added and the amount that actually contributes to the doping level is due to

that fact that most of the Na is located at grain boundaries and on the exterior of the film.

Traditionally, Na is commonly incorporated into the CIGS material by diffusion

from either a layer containing Na that is applied before the CIGS material or from a soda-

lime glass (SLG) substrate [28]. These methods for the addition of Na have some

drawbacks. For example, it can be difficult to get a constant level of Na as SLG is not

perfect in the sense that the amount of Na varies from location to location within the SLG

[28]. Another example is that the Na containing layer must be thick enough to provide

the proper amount of Na without being so thick that the CIGS layer starts to detach [28].

Rudmann et al. [28] developed a new way to add the required Na to CIGS material with a

post-deposition treatment (PDT) of NaF. For the experiment the PDT was applied to

CIGS material that was grown at one of the following temperatures: 400°C, 450°C, or

580°C [28]. The sample with a substrate grown at 400°C had an efficiency of 13.3%

while the sample with a substrate grown at 450°C had an efficiency of 14.4% [28]. Both

samples were tested under an AM1.5 spectrum. For the sample produced at 580°C, the

only comment was that comparable results were achieved [28]. There didn't seem to be

as much emphasis placed on the results of the sample that was processed at 580°C which

was attributed to dissimilar structural properties which were not elaborated on [28]. This

method solves the problems mentioned above and it is also good for adding Na to CIGS

material on flexible substrates such as stainless steel and polyimide which are desired for

use in space [28].

1.4.2   Different Substrates

CIGS based solar cells on flexible substrates are an area of research for space

applications [12]. This is because solar arrays on these substrates can be made to fit in

smaller area and still provide the same amount of power [12]. One such substrate is 0.1

mm thick stainless steel which produced cells with efficiencies of 17.0% and 8.1 % with

and without the addition of sodium under AM1.5 irradiation [29]. As seen, the addition

of Na increases the solar cell efficiency greatly. Other flexible substrates are polymer

and titanium which produce efficiencies of 13.5% and 15.1% [12].

One company has made a totally flexible power system [30]. It was not stated

how flexible the integrated system was, but it was stated that the CIGS based solar cell

can be rolled on a 1 cm diameter roll [30]. This system includes the solar cells, battery

and power management [30]. For purposes of this paper, only the CIGS based solar cell

will be discussed. The solar cell is made up of a CIGS material on a polyimide substrate

[30]. There is no metallization for top contacts [30]. Contact is made by the transparent

indium tin oxide (ITO) layer [30]. A laser is used to define each cell in the material [30].

6

Testing of the cells showed an efficiency of 10.5% with AM1.5 irradiation [30]. Though this is not a very high efficiency, it is valuable research towards flexible CIGS based solar cells and in this case flexible power management system that could be very useful for space applications.

1.4.3 Coatings and Layers

Cadmium sulfide (CdS) buffer layers deposited by Chemical Bath Deposition (CBD) play many roles in CIGS based solar cells according to Rau and Schock [15]. One of the more important roles is that it helps to restore a positive charge to the interface which is partially caused by the elimination of the oxide that is formed when the CIGS material is produced thus producing an n-p junction [15]. Other reasons for the importance of the CdS buffer layer are that it protects the CIGS surface from damage from the addition of the zinc oxide (ZnO) layer that is applied after the CdS and that it covers up the rough surface of the CIGS material [15].

Research has been completed to find a replacement for CdS. It should be noted that all experiments were conducted under AM1.5 conditions except those of Platzer-Bjorkman et al. [31]. This is due to environmental reasons as CdS is a very toxic element and higher band-gap energy materials such as this will help to increase current output [16], [32], [33], [34]. In an effort to replace CdS buffer layers, several different materials have been investigated, but four that stand out are: In_2S_3, Zn (O,S), ZnS, and ZnS (O,OH) which produced efficiencies of 16.4%, 16.0%, 17.7%, and 18.6%, respectively [16], [31], [32], [35]. Very little information was given about the processing and specifications of the CIGS material when these buffer layers were tested [16], [31], [32], [35]. When compared to cells with efficiencies above 19% which belong to the highest efficiency

cells with a CdS buffer layer, it can be seen that there are some materials such as ZnS (O,OH) which could easily replace CdS as a buffer layer [36].

ZnO is an anti-reflection (AR) coating which eliminates much of the reflection for a targeted wavelength of incident light [1]. This is done by adjusting the thickness of the AR coating so that a phase difference of $\pi/2$ is generated at the targeted wavelength [1]. The AR coating material is chosen based on its refractive index which needs to be flanked by the values of free space and that of the CIGS material [1]. In the research by Contreras et al. [16], the ZnO layer is referred to as a window layer. Window layers have a larger band-gap energy compared to the absorber material used within the cell [1]. An example would be the band-gap energy of CIGS and ZnO which are 1.15 eV and 2.4 eV, respectively [25]. As seen, the potential of the ZnO layer is much larger than that of the CIGS and is used to keep electrons within the cell and away from the surface [1]. When this is done, the cell has a higher efficiency [1].

1.5 Radiation Degradation

Charged particle radiation causes severe damage to solar cells limiting their useful time in space [9], [37]. Solar protons (hydrogen ions) and atomic oxygen cause large numbers of vacancies, which act as recombination centers at deep levels and can also create compensating defects that reduce the acceptor concentration at shallow levels [9], [38]. Other sources of damage to solar cells are plasma discharges, atomic oxygen, and electron radiation [12]

There have been many different efforts made to solve and understand this problem. Two main things have been done in an effort to deal with radiation degradation to date. First, how much power the satellite will need and how long it must be in

operation in space must be known [9]. The idea is to make the solar array larger than necessary so that after a given amount of time and radiation degradation, enough power will still be generated at the End of Life (EOL) of the satellite [9]. The next thing that is done is to use a cover-glass over crystalline solar cells [17]. By using the proper thickness and type of cover-glass, a large portion of the radiation damage occurs within the cover-glass and not the solar cell [17]

Another action that has been taken is to use different materials and structures such as 3 and 5 junction cells made from III-V materials and CIGS [11], [37], [39], [40], [41], [42], [43]. At first GaAs was used, but it was found that more complex triple junction devices such as GaInP/GaAs/Ge are more resistant to radiation [9], [11]. Another approach taken by Morioka et al. [44] showed that AlInGaP made a better material for the top cell compared to the traditional InGaP material. It has also been found that cells with more junctions, such as the 5 junction AlGaInP/GaInP/AlGaInAs/GaInAs/Ge cells, have even better radiation resistance [39]. In this case, the aforementioned 5 junction cell had a higher remaining factor of its power (93%) as compared to a 3 junction GaInP/GaInAs/Ge cell (88%) [39]. A second material that has been studied for its radiation hardness is indium phosphide (InP). Indium phosphide is more resistant to radiation hardness than GaAs which is due to the fact that damage caused by radiation can be annealed from InP under the proper conditions [40]. The last new material of interest is CIS based cells such as CIGS. CIGS is very radiation resistant as damage can be annealed from the absorber material [13], [37]. Due to the results of a model developed by Kawakita et al. [13], it is believed that a cover-glass is not necessary for CIGS based solar cells. In general this would have the effect of requiring less material to

build the solar cell which would make it lighter and less expensive to deploy in space and reduce manufacturing costs.

Another aspect to improving radiation resistance of solar cells is to improve a given cell. One example can be seen by the modeling and experimentation of Yamaguchi et al. [45], where it was found that increasing the doping concentration in the base of a silicon solar cell increases the end of life efficiency providing the electron fluence is above 10^{16} cm^{-2}. Another such example of this is that if one decreases the thickness of an InP cell the radiation resistance is increased [41]. This is due to the fact that the diffusion length, though degrading due to radiation, is still larger than the base thickness [41]. It was also found that increasing the amount of Si used as a dopant can increase the electric field between the junction and the surface of the solar cell thus causing a drift current rather than a diffusion current [43]. The increased amount of Si was also found to decrease the series resistance and increase the efficiency [43].

Large amounts of modeling and experimentation have been completed to date on many types of solar cells in order to better understand and protect against the effects of radiation. By understanding more about the damage caused by charged particle irradiation and being able to protect against it, solar arrays can stay deployed longer and the size of solar arrays can be minimized and still ensure adequate power at the end of a satellites life [9]. The preceding was a brief look at various efforts made. Modeling and experimentation results for CIGS based solar cells are reviewed in the next chapter. In the rest of this paper, a new model for proton degradation of CIGS solar cells will be discussed.

CHAPTER 2 PRESENT RESEARCH

Much work has been completed studying the effects of proton irradiation on CIGS

solar cells. In the following sections, information learned from various modeling efforts

and experimental results will be reviewed.

2.1   SRIM Simulations

SRIM (the Stopping and Range of Ions in Matter) by Ziegler et al. [46] is

freeware which calculates the final locations of incident ions as well as the damage,

creation of phonons, and ionization damage due to incident ions [47]. Understanding the

location of the vacancies produced is important so one can determine how much damage

particular proton energies are going to cause the solar cell in question [48]. Depending

on the proton energy, very few vacancies may be created within the cell, or there may be

great numbers of vacancies within the junction causing damage to the cell parameters

which tends to be at a maximum with 300 keV protons [48]. With lower energy protons

the bulk of the damage is created at the front of the cell, while with higher energy protons

the majority of the damage is created toward the back of the cell [49]. Protons cause the

greatest number of vacancies at the point before they stop within the cell [49]. Woodyard

[48] performed SRIM simulations and found that 40 keV protons had a range and

straggle of 0.43 μm and 0.12 μm and 350 keV protons had a range and straggle of 2.71

μm and 0.22 μm for a given cell structure. It should be noted that the values for range

and straggle are for one cell structure and can change using different materials and

structures [49]. Above a certain proton energy, which depends on the solar cell in

question, protons are of high enough energy to travel completely through the cell mostly

creating ionization damage [49].

2.2   Modeling

There have been many modeling efforts of the effects of proton irradiation on CIGS based solar cells completed to date. The first thing necessary for a model is to be able to know various physical constants for the CIGS layer. Such constants are the effective density of states in the conduction and valence bands (N_c and N_v), hole concentration (p), the band-gap energy (E_g), and the electron and hole mobilities (μ_e and μ_h) which are detailed in Gloeckler and Farenbruch [25] and Rockett [26].

Several different computer programs were used by various researchers to model the proton damage to CIGS based solar cells. One of the most commonly cited models used to calculate the number of protons at various energies required for the simulation is the AP8-Max model which is part of SPENVIS, developed by the European Space Agency [50]. It should be noted that the AP8-Max model was originally developed by the Aerospace Corporation and models the proton flux at a chosen orbit during solar maximum [51]. The following programs are not used for calculating the damage caused by proton irradiation, but are used more for general modeling and would be useful to calculate various attributes such as V_{oc} and I_{sc} after information about damage due to irradiation was already determined using a program such as SRIM. One such program that is used extensively, including the work done by Rockett [26], is AMPS which stands for Analysis of Microelectronic and Photonic Structures, developed at the Pennsylvania State University [52]. Although there are other computer programs available such as SCAPS and ADEPT, the AMPS software is the most frequently cited [26].

Several other researchers have completed work concerning the degradation of CIGS solar cells due to radiation damage. First, there is a model which uses the number

of displacements to predict the drop in maximum power [53]. A calculation of the displacement damage dose was completed, which is determined by multiplying the fluence by a constant referred to as the NIEL (nonionizing energy loss) [53], [54]. In order to get the proper curves, experimental data was used to obtain the proper coefficients [53]. One option is to include the effects of annealing into the model [53]. This allows the user to determine how much the cell will actually degrade versus a "worst case" situation where there is no annealing of the damage within the solar cell [53]. The goal of this model was to be able to predict the remaining power after irradiation of this type of CIGS solar cell without having to perform further experimentation [53].

Other models include relative and absolute damage coefficients which are used by Boden et al. [49]. The relative damage coefficient is based on experimental results and uses the fluence at which a given parameter is degraded to a certain point and normalizes it in this case to the same fluence for 1MeV proton irradiation, thus producing a damage coefficient of 1 for 1 Mev protons [49]. Using this method, the maximum damage was found to be at about 500 keV for the cell material tested [49]. Next, there is the absolute damage coefficient for thin film cells which is a proportionality constant between the percentage that a solar cell parameter changes and the proton fluence [49]. Using this method, the maximum damage was again shown to occur at about 500 keV [49].

A model by Kawakita et al. [13] predicts the remaining factor of the open-circuit voltage and the short-circuit current. This model is a fit to experimental data obtained from the flight of the MDS-1 satellite [13]. Though this model shows an accurate depiction of the degradation of the open-circuit voltage and short-circuit current, it lacks insight into why the degradation of these parameters occurs.

Jasenek and Rau [38] present a numerical model to calculate the change in the number of defects, the open-circuit voltage and the saturation current density for a given fluence of either protons or electrons. An important step is to determine the defect introduction rate. In order to do this, a value for the initial defect density, determined experimentally, divided by the defect introduction rate is determined from experimental results [38]. The next step is to calculate the value of ΔV_{oc} where the number of defects has doubled which is also where V_{oc} starts to change [38]. After a value for ΔV_{oc} is calculated, it can be used with the quotient of the initial defect density and defect introduction rate to calculate the actual defect introduction rate [38]. The other important input parameter is the initial defect concentration which was determined using defect spectroscopy and was determined to have a value of 4×10^{15} cm^{-3} [38].

2.3   Experimental Results

Many experiments have been done to determine the effects of proton irradiation on CIGS solar cells. The first one of interest used a CIGS solar cell that was aboard the MDS-1 satellite that was launched in February 2002 [37]. It should be noted that there were a total of eight different types of cells that were aboard the satellite on a test fixture [37]. Of each type of cell, there were two cells each with either a 100 or 500 mm cover glass with only one exception, the GaAs/Ge cells [37]. Though the test was comprised of solar cells that were not developed for space use, it is a valuable insight into the response of CIGS solar cells to proton irradiation [37]. One important finding was that the CIGS cells showed very little degradation compared to other cells including crystalline silicon cells that were manufactured for space [37]. This is mostly due to the ability of defects

14

within the CIGS layer to be annealed, which could happen at temperatures as low as about 70°C [37].

There have been many lab tests on CIGS solar cells completed and there are several notable findings. First, lower energy protons cause more damage to the solar cells than higher energy protons [48]. One example of this is where a test performed by Kawakita et al. [13] showed that the open-circuit voltage, V_{oc}, was strongly degraded by 0.38 MeV and 1 Mev protons as compared to protons of higher energies. Another interesting fact shown was that higher energy 1 and 3 Mev protons caused more damage to the short-circuit current, I_{sc}, than the 0.38 MeV protons [13]. In experiments conducted by Jasenek et al. [55], 290 keV protons caused more damage for all solar cell parameters than the 1 and 10 Mev protons which were also tested. The interesting fact here is that Kawakita et al. [13] had more degradation of I_{sc} for 1Mev protons and less for the 0.38 Mev than did Jasenek et al. [55]. It should be noted that protons with too low of an energy will not affect the solar cell output as protons will not penetrate through the window layer as noted by Kawakita et al. [13]. It was also noted by Jasenek et al. [55] that lower energy particles between 100 and 500 keV will tend to cause damage in one part of the cell, whereas higher energy protons will tend to cause damage throughout the cell.

Another consideration that must be taken into account when discussing the results of experiments is the temperature at which they were conducted. It was shown by Kawakita et al. [56] that the amount of degradation is higher at lower temperatures for the same proton energy and fluence. Another effect of temperature is thermal annealing [13]. Experiments conducted by Kawakita et al. [56] showed that the recovery of I_{sc} and V_{oc}

was greater at higher temperatures. Thus, it is also sometimes necessary to run experiments at a lower temperature to make the effects of annealing negligible [13].

It was noted by Boden et al. [49], that losses in V_{oc} and the fill-factor, FF, cause the majority of the loss of efficiency, η. It was also noted by Weinert et al. [57], that as the proton fluence increases, changes in I_{sc} play more of a role in degrading the efficiency. The decrease in the FF , which describes how "square" the current-voltage curve is, was noted by Jasenek and Rau [38] to be mostly caused by two factors which were increases in the diode ideality factor and the series resistance, but the diode ideality factor didn't become an issue until higher fluences were obtained [2]. Other than this, it was stated by Jasenek and Rau [38] that more work would be required for a better explanation of the drop in the fill-factor.

2.4   Differences between Present Research and the Proposed Model

There are only a few differences between what has been previously done with SRIM and the work described here. One of the biggest differences is that the values for binding and displacement energies were not altered from the pre-set values as they were by Weinert et al. [57]. Another major difference in simulations completed by Weinert et al. [57] and Woodyard [48] is that protons enter at 90 degrees to the solar cell where this project uses protons entering at a wide variety of entry angles. Simulating protons with varying entry angles has probably been completed using SRIM in the past on other materials as it is clearly stated how to complete this in the SRIM Instruction Manual [47], but no reference to doing this was found in any publications concerning CIGS solar cells. The final notable difference is in the method of calculating the defect introduction rate, γ. Weinert et al. [57], calculate the defect introduction rate by multiplying the number of

16

vacancies created by each proton, N_p, with the thickness of the CIGS layer yielding units of cm^{-1}. In order to compare the methods of Weinert et al. [57] and those used in this project for calculating the defect introduction rate, a TRIM (the Transport of Ions in Matter) simulation was completed [47]. The TRIM simulation used the same cell structure as well as displacement and binding energies outlined by Weinert et al. [57]. The defect introduction rate was then calculated using the method used for this project as described in the next chapter. Defect introduction rates of 1.32 x 10^5 cm^{-1} and 1.25 x 10^5 cm^{-1} were obtained after 2006 and 8031 incident protons where the value of $\gamma = 1.32$ x 10^5 cm$^-$1 is the same as produced by Weinert et al. [57]. The method for calculation of γ presented by Weinert et al. [57] seems very tedious and was difficult to follow which leads to the recommendation of the method used in this project due to the fact that γ is very simple and quick to calculate.

An additional difference is that not as many detailed constants are needed as in the publications by Gloeckler and Farenbruch [25] and Rockett [26]. For this project, only the following information is needed:

- Initial open-circuit voltage

- Initial short-circuit current or current density

- Area and thickness of the sample

- Band-gap Energy

- Electron and Hole Mobilities in CIGS layer

- Effective Density of States of Conduction and Valence Bands

- Hole Concentration

- Introduction Rate of Compensating Defects

Another major difference was the software that was used. Besides the use of SRIM, MS Excel, Mathcad and MATLAB, all programs were written by the author. When using this model, proton irradiation experiments are not required for different structures as they are in the article by Walters et al. [53] or Boden et al. [49]. Boden et al. [49] seem to say that their model will work on any CIGS cell for any radiation damage, but it is not clear. Based on the results of Boden et al. [49], it seems that their model is only applicable to one type of CIGS solar cell and if any changes are made as far as thickness, composition, structure, or any other attribute, it would be necessary to perform radiation testing again so that the model may be changed as necessary. It should also be noted that the model that is used for this project provides the actual and normalized amount of the remaining open-circuit voltage, short-circuit current, fill-factor and efficiency with respect to the proton fluence without having to convert back and forth to displacement damage dose.

Equations used for the total number of defects and the change in V_{oc} from Jasenek and Rau [38] were used. However, standard equations were used for the calculation of other parameters such as the fill factor and the efficiency. The only equation that was derived by the author, as a fit to experimental data, was that for the degradation of the current. Equations used in the proposed model are discussed in more detail in the next chapter.

The proposed model for CIGS based solar cells will provide a method of calculating the remaining factors of cell parameters and requires fewer inputs, requires little initial testing and provides a more realistic model than many existing models.

CHAPTER 3 METHODOLOGY

The goal of this project is to model the effects of different energies and fluences of protons on CIGS solar cells. In the following sections, the theory, mathematics and computer software used in this model are discussed.

3.1 Theory

The goal of this project is to calculate the effects of proton irradiation at different energies on the open-circuit voltage (V_{oc}), short-circuit current (I_{sc}), fill-factor (FF) and the efficiency (η) of CIGS solar cells. The first step is to calculate the defect density after a proton fluence (ϕ) which is done using equation 1 [38].

$$N(\phi) = N(0) + \gamma\phi \qquad (1)$$

where N(0) is the initial defect density with a value of 4×10^{15} cm^{-3} as determined through experimentation and modeling by Jasenek and Rau [38] and γ is the defect introduction rate [38]. The defect introduction rate is determined using the information provided in the vacancy.txt file produced by SRIM. Information for each element in each layer of the solar cell is listed with the number of vacancies/Ion/Angstrom listed at each depth where the depth of the solar cell is divided into 100 equal segments. In order to get the defect introduction rate, the first steps are to sum the number of vacancies at each depth and to multiply the sum by 10^8 to obtain units of vacancies/ion/cm. Next, an average of the vacancies at each depth is taken. This value is used for the defect introduction rate (γ)

The next step in the model is to find the values of V_{oc} and I_{sc} after proton irradiation. The importance of V_{oc} and I_{sc} is that they provide the maximum attainable voltage and current achievable by the solar cell [58]. In order to find V_{oc} we used equation 2 which was derived by substituting an equation for the saturation current as a

19

function of defect density, equation 3, into the general equation for V_{oc}, equation 4, and equation 1 is then substituted in to take into account the defect density after a proton fluence, ϕ [38]. Last of all, equation 5 is used to determine the change in V_{oc} and produce the final form of equation 2 [38]. For full details of the derivation, the reader is referenced to the work of Jasenek and Rau [38].

$$\Delta V_{oc} = \frac{AkT}{q} \ln(1 + \frac{\gamma\phi}{N(0)}) \qquad (2)$$

$$j_o = \frac{n_i \pi kT}{|F_{max}|} \sigma v_{th} N \qquad (3)$$

$$V_{oc} = \frac{KT}{q} \ln(\frac{j_{sc}}{j_o} + 1) \qquad (4)$$

$$V_{oc}(\phi) = V_{oc}(0) - \Delta V_{oc}(\phi) \qquad (5)$$

In the previous equations, A is the diode ideality factor, F_{max} is the value of the maximum electric field, σ is the capture cross section, and v_{th} is the thermal velocity where a value of 10^7 for electrons was used as presented by Gloeckler, et al. [25], [38]. Last of all, it should be noted that $V_{oc}(0)$ is the initial value of V_{oc} before irradiation and $V_{oc}(\phi)$ is the value of V_{oc} after a fluence, ϕ, of proton irradiation [38].

The next step is to calculate the normalized open circuit voltage which shows the remaining factor of the open-circuit voltage and is easily computed using equation 6.

$$V_{oc-Normalized} = \frac{V_{oc}(\phi)}{V_{oc}(0)} \qquad (6)$$

Being able to calculate an accurate value for I_{sc} is very important as it is one of the main parameters used to judge the performance of a particular solar cell and it is used in many of the calculations for other parameters such as the fill-factor and efficiency.

The short-circuit current is the only value that was determined using a fit to experimental data. Several other approaches were attempted to calculate the value I_{sc}, but did not provide reliable results as will be discussed in the results section. A basic approach to calculate the value of the short-circuit current was to have an exponential decay of the initial value which is of the form:

$$I_{sc}(\phi) = (J_{sc}(0)A)\exp(\frac{-\alpha\phi}{J_{sc}(0)}) \qquad (7)$$

where J_{sc} is the short-circuit current density, α is a constant depending on the energy of the incident protons, and A is the area of the cell being tested. The value α has no physical meaning except to help define the rate of decay of short-circuit current at a given proton energy. Values for α at different fluences were calculated by trial and error for the first set of simulations which are presented in the next chapter. From the three values of α obtained in the first set of simulations, Mathcad was used to fit a curve using the pwrfit() function. A curve of the form $a*x^b+c$ was obtained with $a = 4.834x10^{-4}$, $b = 0.768$, and $c = 0.136$ and x is the defect introduction rate. It should be emphasized that the first set of simulations were used to determine values of α that were then used in Mathcad to produce the plot of α vs. γ which can be seen in Figure 3-1. Values of α in the second set of simulations were obtained by using the plot produced by Mathcad. The normalized value of the short-circuit current was calculated using an equation similar to equation 6.
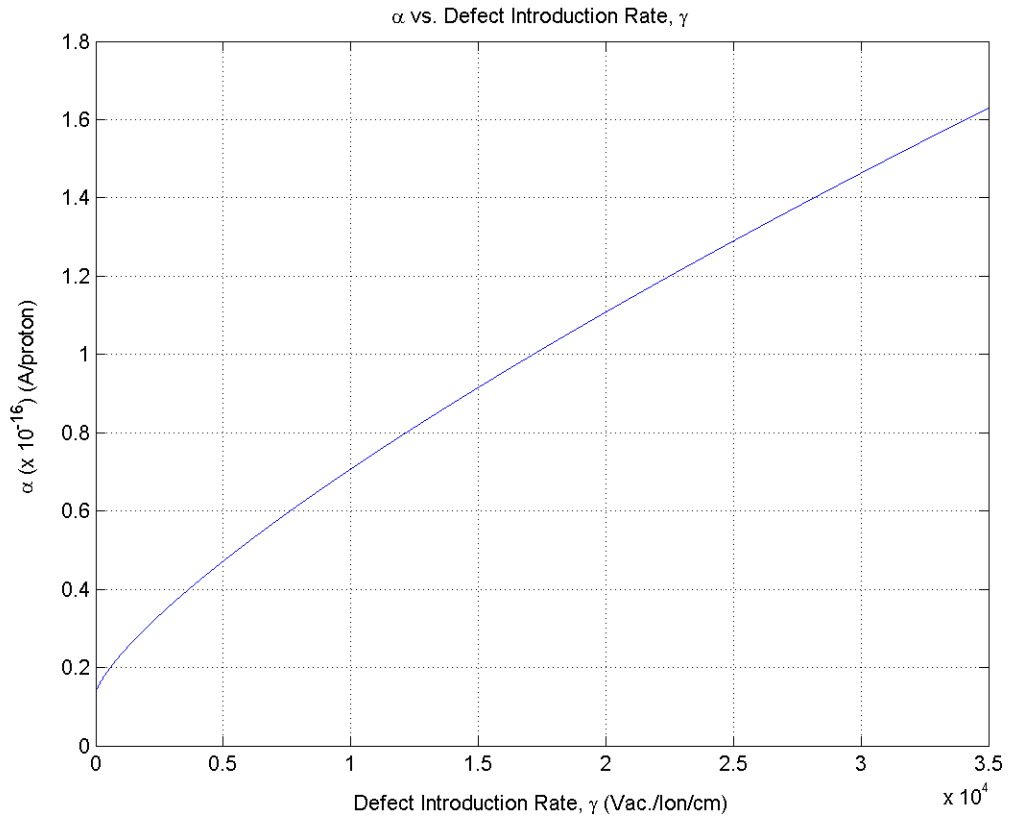
Figure 3-1 – Plot of the α vs. Defect Introduction Rate, γ.

The remaining solar cell parameters that need to be calculated are the fill-factor (FF) and the efficiency (η). The fill factor describes how "square" the current-voltage curve is [2]. It is determined by the maximum voltage and current points, V_{mp} and I_{mp}, which represent the maximum output power of the solar cell [2]. When the maximum power point is translated to the voltage and current axes, a square is made [1]. The ratio of the area of this square to the area of a square made by the V_{oc} and I_{sc} points gives the fill-factor [2]. Last of all, the efficiency is a ratio of the output power to the input power providing a fraction of how much of the incident solar power was converted into electrical power [1].

In order to calculate the fill-factor, the maximum-power voltage and current, V_{mp} and I_{mp} respectively, must first be found. In order to calculate V_{mp}, the saturation current must be found. In order to do this, equation 8 was solved for the saturation current I_o to obtain equation 9 [2]. Although other methods of calculating I_o were attempted, which are discussed in the next chapter, this method produced the best results.

$$V_{oc} = \frac{KT}{q} \ln(\frac{I_{sc}}{I_o} + 1) \qquad (8)$$

$$I_o = \frac{I_{sc}}{\exp(\frac{V_{oc}q}{kT}) - 1} \qquad (9)$$

Next, V_{mp} can be solved for recursively using equation 10 as this value cannot be solved for explicitly [59]. This result is then used in equation 11 to solve for I_{mp} [58].

$$V_{mp} = V_{oc} - \frac{kT}{q} \ln(\frac{V_{mp}}{(kT/q)} + 1) \qquad (10)$$

$$I_{mp}(\phi) = I_{sc} - I_o(\exp(\frac{qV_{mp}}{kT}) - 1) \qquad (11)$$

At this point there are only two basic cell parameters to calculate, the fill-factor and the efficiency. First, a value for the series resistance for the cell is needed. To calculate the series resistance, the doping level of acceptors (N_A) after the proton fluence must be calculated first. In order to calculate N_A, equation 12 is used where $N_A(0)$ and $N_A(\phi)$ are the values of the doping density before and after proton irradiation, and γ_c is the rate at which compensating defects are introduced and has units of cm^{-1} [38]. The values for the rate at which compensating defects are introduced were found by trial and error so the results would resemble those of Jasenek et al. [55]. The three values used for the first set of simulations were input into Mathcad where the pwrfit() function was used to determine three coefficients for an equation of the form $a*x^b + c$ where a = 376.023, b = 0.216, and c = -1.938x10^3 and x is the defect introduction rate.

$$N_a(\phi) = N_a(0)\exp\left(\frac{-\gamma_c\phi}{N_a(0)}\right) \qquad (12)$$

The value of γ_c is not a given constant. Jasenek and Rau [38] attempted to measure this value by experimental means but were only able to estimate a value of greater than 5000 cm^{-1}. Though it is not stated clearly, it is understood that the γ_c obtained is only for 4 MeV protons. Through a method of trial and error, values of 1650 cm^{-1}, 1050 cm^{-1}, and 0 cm^{-1} were obtained for proton fluences of 290 keV, 1 MeV, and 10 MeV, respectively. This makes sense in the fact that more compensating defects will be created with 290 keV versus 1 MeV or 10 MeV irradiation and thus the acceptor concentration will decrease more after 290 keV proton irradiation. The problem with the

methodology just mentioned is that there is no experimental or mathematical backing for the values of γ_c obtained. A plot of γ_c vs. γ can be seen in figure 3-2. Next, the resistivity can be calculated using equation 13 which is a standard equation which has units of Ω-cm [2]. Now the series resistance of the solar cell is found by multiplying the resistivity by the thickness of the CIGS layer divided by the area of the solar cell as seen in equation 14 [58]. The previous result can then be normalized by dividing by the characteristic resistance as seen in equation 16 [2]. The characteristic resistance is defined as the open-circuit voltage divided by the short-circuit current as shown in equation 15 [2]. At this point, the fill-factor can be calculated using equation 17 and then corrected for the effects of series resistance using equation 18 [2]. The fill-factor can be normalized in using the same method as V_{oc} and I_{sc}.

$$\rho = \frac{1}{q\mu_e N_D + q\mu_h N_A} \qquad (13)$$

$$R_S = \rho \frac{Thickness}{Area} \qquad (14)$$

$$R_{ch} = \frac{V_{oc}}{I_{sc}} \qquad (15)$$

$$r_{series} = \frac{R_s}{R_{ch}} \qquad (16)$$

$$FF(\phi) = \frac{V_{mp} I_{mp}}{V_{oc} I_{sc}} \qquad (17)$$

$$FF_{series}(\phi) = FF(\phi)(1 - r_{series}(\phi)) \qquad (18)$$

The final calculation that needs to be made is that of the efficiency. This is completed using equation 19 shown below where P_{in} is the input power at Air Mass 1.5

which has a standard value of 1000 W-m^{-2} [1], [2]. It should be noted that AM0 test conditions with an input power value of 1367 W-m^{-2} should be used in most situations [3]. The value for the input power can be changed by altering the CIGS Calculator program that will be discussed later in this chapter. AM0 conditions were not used in this case as the experimental data by Jasenek et al. [55] used AM1.5 test conditions.

The normalized efficiency can be calculated in a similar manner to that of the open-circuit voltage as shown in equation 6.

$$\eta(\phi) = \frac{V_{mp}(\phi)I_{mp}(\phi)}{P_{in}} \qquad (19)$$
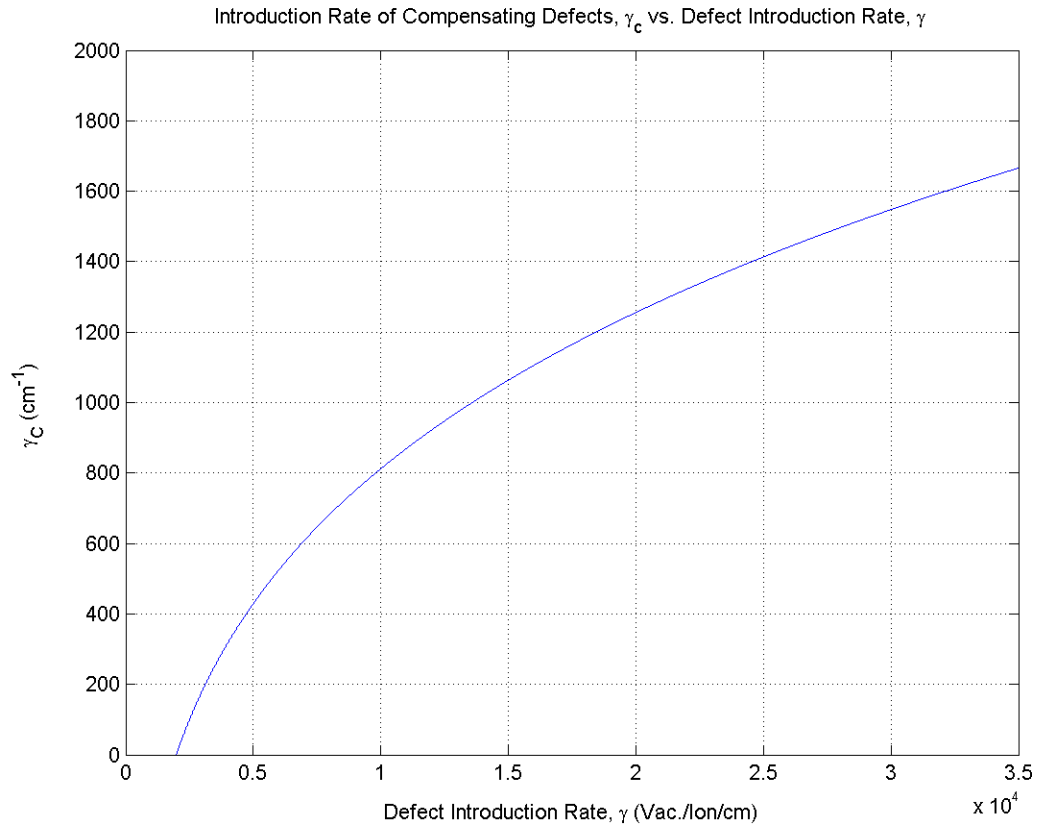
Figure 3-2 – Plot of the introduction rate of compensating defects, γ_c, vs. the defect introduction rate, γ

3.2   Software

In order to complete this model, four different software packages were required:

DataBuilder, SRIM 2006, MS Excel, and CIGS Calculator. DataBuilder and CIGS

Calculator are custom programs written by the author to complete different aspects of the

project where there were no known previously developed software packages available.

In the following sections, descriptions of what was done with each program, and in the

cases of the DataBuilder and CIGS Calculator programs, how they were constructed is

presented.

3.2.1   DataBuilder

A program named DataBuilder was created to generate a text file listing incident

ions and their various attributes which is used as input to SRIM 2006. Though the use of

DataBuilder is not a necessity, it allows the users to avoid writing thousands of lines of

code themselves. DataBuilder is a console application written in Visual C++ using MS

Visual Studio 2005 and the programming code can be seen in Appendix A. It consists of

three basic files which are Driver.cpp, DB.h, and DB.cpp.

Driver.cpp is the highest order part of the program.   There are only three different

tasks that are completed within this file. The first is to write a header to the screen with

the name and author of the program. Second, is to make an instance of the DB class.

Third, the Write() function, which will be described later, is called from within the DB

class.

The file DB.h contains definitions of variables and functions used in the class

which are separated between private and public items. Private items are items which can

only be used by that class whereas public items may be referenced by other functions from outside the DB class.

DB.cpp contains four different functions which do the majority of the work. The first function is the constructor for the DB class which is called when an instance of the DB class in Driver.cpp is defined. In this case, all that occurs is that all of the variables are created which are listed in DB.h, and the "FillPos" and "FillAngle" functions are called. The "FillPos" function fills a vector with numbers between -5000 and 5000 which are in units of Angstroms. These values represent positions in the y and z directions that will be used to define the entry point of each ion. The "FillAngle" function fills a vector with angles between 0 and π radians which will be used to define the entry angles of each ion.

The last function in the DB class is the Write() function. This function creates an output file named trim.dat. Should the computer not be able to make the output file, a message saying "no file" is displayed and the program is terminated. If the output file is created, the program first asks for several inputs which are:

- Number of ions to be simulated.

- Seed value for the random number generator.

- Date the file is created (Optional – may be left blank).

- Energy of the incident ions.

- Atomic number of the incident ions.

- Three lines of comments which can be used or left empty (Optional – may be left blank).

- Stoichiometry of the target (Optional – may be left blank).

29

Once these items have been entered, the program writes the header to the trim.dat file with the following information:

- Date file was created

- Three lines (100 characters each) for comments

- Stoichiometry of the target

- Column headers for the rest of the file

Next, the Write() function has a loop which writes the data for each ion to the trim.dat file. The first thing to happen within the loop is to randomize the values of the position and angle vectors in an effort to simulate the random nature of the ions that are bombarding the target. In order to do this, three different things have been done. First, the vectors that contain the position and angle values are shuffled using a random shuffle algorithm built into C++ which occurs after every five iterations through the loop. Second, the random number generator is seeded with the value that was entered earlier by the user and is incremented after every iteration through the loop. Next, the rand() function is used to pick random values of each angle and the y and z positions. Then the information for each ion is written to the trim.dat file as outlined in [47]. The information listed for each ion is as follows:

- Number of each event

- Atomic number of the ion hitting the target

- Energy of the ion

- Starting position of the ion (x, y, and z coordinates)

    o X coordinate is always 0 meaning it hits at the surface.

- Direction of the ion (uses directional cosines)

30

The final step within the Write() function is to close the output file. After this is

completed, the program is completed and exits. Once the program is complete, the newly

created trim.dat file is ready to be used for simulations using the SRIM 2006 program.

3.2.2 SRIM 2006

SRIM 2006 was used to run the simulations of the ions incident on the target and

is available for free download for non-commercial use. SRIM 2006 calculates the range

and straggle of ions incident on a particular target. This functionality is used in another

program within SRIM called the Transport of Ions in Matter (TRIM). TRIM provides

much information about the bombardment of different materials with ions including the

distribution of ions within the target material and damage to the target material.

First the proper information must be entered into the TRIM program. The

following is a list of the information that can be entered and the options that can be

selected from the main window.

- Ion Data which includes the symbol, name, energy, atomic number, mass, and
  angle of incidence of the ion.

- Target Data which includes the name for each layer, layer width, layer density,
  elements for each layer, and the stoichiometry of the different elements that form
  a layer.

- Select from several different output files that show different results. Some of
  these files are chosen on the first screen where you enter all of your information
  and the rest can be selected from a second screen that comes up and displays
  information while the simulation is running.

- Plotting window depth controls allow you to only view a small part of the target or a larger area if desired.

- The damage menu allows you to choose between different types of calculations that are available.

- There are four basic plots as well as many more specialized plots that are available. The four basic plots show distribution of ions on different planes which can be selected either from the main screen from the pull down menu before the simulation starts or after the simulation starts on the second screen. Other plots that are available may be chosen from the second screen while the simulation is running.

For a full listing of the functionality of the TRIM program, the reader is encouraged to view the SRIM Instruction Manual [47].

To run the simulations, the first thing needed was to place the trim.dat file into the SRIM 2006 folder (or folder where the SRIM program resides). Next, the information for each layer of the target that will be used during the simulation as well as the energy of the ions was entered into the "Ion Data" part of the screen. It should be noted that the energy listed here must be higher than any energy listed for any ion in the TRIM.DAT file or the program will produce an error stating that the particular ion will be skipped because the energy listed in the TRIM.DAT file is larger than the energy in the TRIM.IN file. The TRIM.IN file contains the value for the ion energy entered by the user in the "Ion Data" portion of the screen. In the "Damage" pull-down menu, the selection of "Varying ion energy/angle/depth (full cascades) using TRIM.DAT" was made. All other options on the first screen may be used at the discretion of the user, but are not necessary

for this project. Once the simulation has started and the second screen has appeared, there will be a small window labeled "Plots." In the bottom portion of the Plots window, there will be a sub-section labeled "Distributions" with several options below it. Next to each option there are buttons for files and check-boxes for plots that the user may wish to use. While the simulation is running, the button for creating a file for "Damage Events" needs to be clicked using the mouse. What this will do is to create three files, one of which will be vacancy.txt. In this file, the thickness of the target material is divided into 100 equal pieces. The vacancy.txt file contains an averaged number of vacancies/Angstrom/ion for each element for each of the 100 divisions of the thickness [47]. This data within the vacancy.txt file will be analyzed using MS Excel to find the defect introduction rate in one of the later programs.

3.2.3   Microsoft Excel

The data within the file vacancy.txt produced by SRIM now needs to be analyzed using MS Excel. First, the *.txt file was converted into a Microsoft Excel Worksheet which is easily done by opening the text file and using the Text Import Wizard in Excel. Now the data may be saved as a Microsoft Excel Workbook (*.xls) and manipulated. Next, extra data that was not needed for the calculation of the number of vacancies in the CIGS layer, which includes all of the information in the header as well as information about each element in each of the layers other than the CIGS absorber layer, was removed. After this is completed, all that is left is five columns of information which includes the depth and the number of vacancies/Angstrom/ion for each of the four elements in the CIGS layer.

For the calculations, first we sum up the number of vacancies at each depth. Next, we multiply by 10^8 to convert the units of vacancies/ion/angstrom to vacancies/ion/cm. Third, MS Excel was used to come up with an average of the amended data which is done by using the average function which is built in to MS Excel. This value is the defect introduction rate which will be used in the model to calculate various cell parameters using the CIGS Calculator program.

MS Excel was also used to convert the *.txt file containing the results of the simulation to an MS Excel worksheet (*.xls) which could then be read by MATLAB. The use of MATLAB will be discussed in a later section.

3.2.4   CIGS Calculator

In order to complete the calculations of the degradation of the cell parameters open-circuit voltage (V_{oc}), short-circuit current (I_{sc}), fill-factor (FF) and efficiency (η), another program, CIGS Calculator, was created. CIGS Calculator was written in Visual C++ using MS Visual Studio 2005 and the programming code can be seen in Appendix B. This program is split into three main parts: the driver for the program, and two different classes which are named calculator and fluence. The calculator class provides the basic structure for running the calculations as well as controlling the user interface while the fluence class does the actual calculations for each value of the fluence (Phi).

In this program, the driver.cpp program is very simple in that it contains only one command which is to create a calculator class. By doing this, a calculator object is instantiated and the rest of the program is contained within the two classes.

When a calculator object is instantiated, the first thing that happens is that all of the variables within the calculator.h file are created and the four functions within the

constructor are called. The first two functions within the constructor are the

printHeader() and getInitial(). These two functions perform the following actions:

- Print a header to the console screen

- Ask the user for the following:

    o Defect introduction rate

    o Beginning fluence for simulation

    o Ending fluence for simulation

    o Number of data points

The information that is collected is set into variables within the class for later use in other

functions.

The next function that is called within the constructor is the openOut() function

whose job is to obtain a filename for the output file from the user and create it. It is

important to include the *.txt ending for the filename otherwise the computer does not

know how to properly open the output file. Once the filename is obtained, the program

creates the output file and checks to make sure that it is created.   If it was not created an

error message saying "NO FILE" is displayed and the program is terminated, otherwise a

header containing the name of the program and column headers are printed to the output

file.

The last function that is called from the constructor is the doCalcs() function.

First, the doCalcs() function performs all of the calculations with the value of Phi

(fluence) set to 0. In order to do this, a fluence object is instantiated which will call the

class constructor where all variables within fluence.h are created and defined as needed.

Second, two functions, setPhi() and setDefRate(), which are members of the fluence

class, are called. These two functions set the value of Phi (fluence) and the defect

introduction rate in variables within the fluence class. Third, the RunCalcs() function,

which is again a member of the fluence class, is called which starts the calculation of the

basic cell parameters which are then printed to the output file. Next, the values of Phi

that will be used to make the calculations of the cell parameters are determined which is

done by subtracting the beginning fluence from the end fluence and dividing it by the

number of data points. Afterwards, the doCalcs() function uses a loop to run through the

calculations for the basic cell parameters at each value of Phi which is done the same way

as before, except that a new member of the fluence class is not instantiated each time. If

the program were to create a new member of the fluence class each time through the

loop, this would clear all previous data from the previous time through the loop and set

everything back to its initial conditions which is valid. But for this instance, it was

decided to reset each variable before it was calculated again. This serves two purposes,

the first is that the fluence class is able to remember the initial values (Phi equal to zero)

of the cell parameters for computation of normalized values eliminating the need to

remember these values within the calculator class which would require additional

functions to continually pass the initial values back to the fluence class. The second

reason is that each variable is cleared right before it is calculated again within the various

functions so that all values are recalculated every time which helps to reduce the chance

of errors occurring in calculations. The final action in the doCalcs() function is to close

the output file.

When the runCalcs() function is called, the first thing that is done is to set various

constants that will be required. It should be noted that $V_{oc}(0)$ must be inserted into the

program code for the computations to work properly. Table 3.1 lists all of the cell

parameters that are calculated, the name of the functions that perform the calculation, and

the order in which the function is called after the runCalcs() function is called.

Most of the above calculations are straightforward in their execution; however

recursive equations are not as straightforward to execute in a computer program as is the

case for the calculation of V_{mp} using equation 10. In order to solve equation 10 through

trial and error, a loop was set up which starts off with V_{mp} being equal to 0.001 and the

equation being set equal to a variable named max instead of V_{mp}. The loop goes through

and increments V_{mp} until V_{mp} and max are equal to each other to approximately four

decimal places.

Table 3.1 - *List of Cell Parameters Calculated, Calling Function, and Order of Calculation.*

Order	Quantity Calculated	Function Name
1	Number of Defects	calcN()
2	Open-Circuit Voltage	calcVOC()
3	Normalized Open-Circuit Voltage	calcNVOC()
4	Short-Circuit Current/Normalized Short-Circuit Current	calcI()
5	Saturation Current	calcDarkI()
6	Maximum-Power Voltage	calcVmp()
7	Maximum-Power Current	calcImp()
8	Series Resistance/Doping Density N_A	calcSeriesR()
9	Fill-Factor	calcFF()
10	Normalized Fill-Factor	calcNFF()
11	Efficiency	calcEff()
12	Normalized Efficiency	calcNEff()

3.2.5 Mathcad

Mathcad was used for performing the curve-fitting for the plots of the defect introduction rate vs. α for use in equation 7 and for the defect introduction rate vs. introduction rate of compensating defects, γ_c which is used in equation 12. This program was not used for the final plotting of the aforementioned plots or the plotting of any other results as it would not produce the desired formats and allow for Greek letters to be used in titles and labels.

3.2.6 MATLAB

MATLAB was used to produce all plots used for this project. This program allowed the use of Greek letters and subscripts to be used in plot titles and labels unlike Mathcad. MATLAB was also able to plot the model results using a logarithmic scale on the x-axis which MS Excel would not do. Also, MATLAB was able to import the results of the modeling when it was contained in an MS Excel worksheet. It should be noted that MATLAB was not used to perform any calculations for this model.

CHAPTER 4 RESULTS

Several simulations were run using the CIGS Calculator model. The goal was to

model the effects of different energies of solar protons to see the effect on the basic cell

parameters V_{oc}, I_{sc}, FF and η. Two different sets of simulations were run in order to

compare the model to two different sources of experimental data. The first simulation

was used to compare the results of the model to the experimental results of Jasenek et al.

[55] and the second to the results of Boden et al. [49].

4.1   Simulation I

This simulation was meant to compare the results of the model to the

experimental results of Jasenek et al. [55]. The proton energies that were used were

290keV, 1MeV, and 10MeV [55]. Results produced by Jasenek et al. [55] were made

using an AM1.5 spectrum. The cell structure that was used by Jasenek et al. [55] is

shown in Table 4-1:

Table 4.1 – *Structure used by Jasenek et al. [55].*

Layer Name	Thickness (Angstroms)
ZnO –doped with Al	3000
ZnO	500
CdS	500
CIGS	1.5-2μm (2μm used in simulation)

First, the DataBuilder program was used to create a list of individual protons that

would be incident on the target. A fluence of 9.99×10^4 protons/μm^2, which is the

equivalent of 9.99×10^{12} protons/cm^2, was used in the simulation. A portion of the

trim.dat file can be seen in Appendix D. The modified MS Excel worksheet showing the calculation of the defect introduction rate of 3.43×10^{4} Vacancies/Ion/cm for 290 keV protons is shown in Appendix C. Last of all the output file from the CIGS Calculator file can be seen in Appendix E. The experimental results from Jasenek et al. [55] are shown in Table 4.2 and may be compared to the simulation results in Table 4.3 and the plots in Figure 4-1. Also, the percentage difference between the experimental results for Jasenek et al. [55] and the simulation results are detailed in Table 4.4. When the percentage difference is a negative number, this indicates that the value obtained by the simulation is larger than the experimental value. It should also be noted that the simulation results are actually at a fluence of 1.10×10^{12} protons/cm^2 rather than 1.0×10^{12} protons/cm^2. This small difference is considered to be negligible for comparison of the results produced by the simulation and those produced experimentally by Jasenek et al. [55]. Primarily, this is because it is difficult to obtain results to that level of accuracy from the plots presented by Jasenek et al. [55]. One last note is that Jasenek et al. [55] used short-circuit current density, J_{sc}, whereas this model uses the short-circuit current, I_{sc}. Though there is a difference in units, the values for the normalized remaining factor are equal, since normalization cancels out the effect of area.

With 290 keV irradiation, the normalized V_{oc} is about 0.83 and 0.51 for fluences of 1×10^{12} protons/cm^2 and 1×10^{14} protons/cm^2, respectively, calculated by the CIGS Calculator model correlate well with experimental results. The only notable difference is that V_{oc} seems to be a little lower than the experimental values which is probably due to the fact that the value of the diode ideality factor, A, used in the calculation, was slightly too small. Also, the 10.53% difference in the open-circuit voltage at a fluence of

41

1×10^{14} protons/cm^2 could be partially attributed to the initial defect density, N(0) that was used in equation 2. The curve for I$_{sc}$ is a fit to the experimental data of Jasenek et al. [55] with the constant α used in equation 7 was 1.6×10^{-16} A/proton. Comparing the normalized values of I$_{sc}$ from [55] at fluences of 1×10^{12} protons/cm^2 and 1×10^{14} protons/cm^2, there is little difference with the values of 0.99 and 0.60 produced by the model. The value of γ_c obtained for use in equation 12 was 1650 cm^{-1}. Results for the normalized fill-factor produced by the CIGS Calculator model agree relatively well with the experimental results of Jasenek et al. [55]. At fluences of 1×10^{12} protons/cm^2 and 1×10^{14} protons/cm^2, the model produced values of 0.97 and 0.40, respectively. Differences in the fill-factor can most likely be attributed to the differences in the calculation of the open-circuit voltage. The difference could also be attributed to the value of γ_c being too high. When γ_c is too high, the acceptor density is too low which causes the series resistance to be too high. The values for the normalized efficiency produced by the model are 0.80 and 0.12 for fluences of 1×10^{12} protons/cm^2 and 1×10^{14} protons/cm^2, respectively, which are both relatively close to the values produced by Jasenek et al. [55]. Overall, it can be seen that 290 keV protons cause extensive damage to the solar cell.

Table 4.2 – *Experimental results from Jasenek et al. [55] for 290 keV protons.*

Fluence	Norm. V$_{oc}$	Norm. I$_{sc}$	Norm. FF	Norm. Efficiency
1×10^{12}	0.85	0.97	0.95	0.77
1×10^{14}	0.57	0.60	0.42	0.12

Table 4.3 – *Simulation results for 290 keV protons.*

Fluence	Norm. V_{oc}	Norm. I_{sc}	Norm. FF	Norm. Efficiency
$1x10^{12}$	0.83	0.99	0.97	0.80
$1x10^{14}$	0.51	0.60	0.40	0.12

Table 4.4 – *Percentage difference between Jasenek et al. [55] and simulation results for 290 keV protons.*

Fluence	Norm V_{oc}	Norm. I_{sc}	Norm. FF	Norm. Efficiency
$1x10^{12}$	2.35%	-2.06%	-2.11%	-3.90%
$1x10^{14}$	10.53%	0%	4.76%	0%
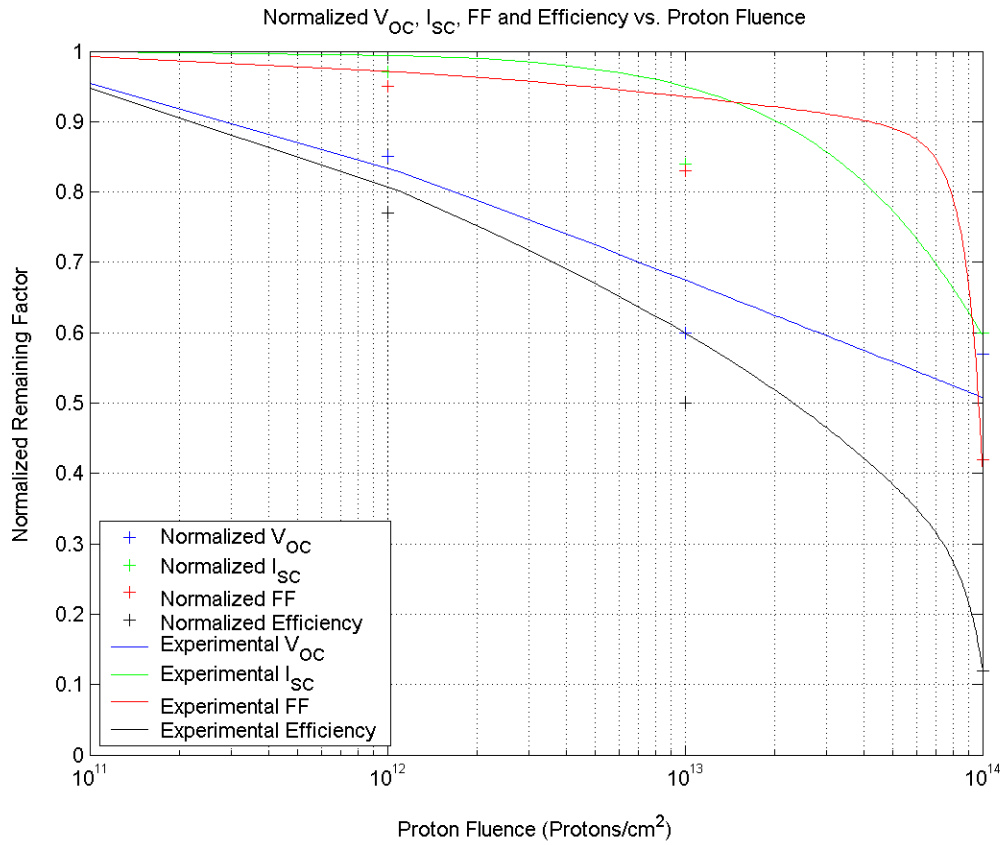
Figure 4-1 - Normalized open-circuit voltage, short-circuit current, fill-factor, and efficiency for 290 keV proton irradiation. Experimental results are those of Jasenek et al. [55].

Experimental results, simulation results, and percentage difference between the two sets of results for 1 MeV proton irradiation are presented in Tables 4.5, 4.6, and 4.7. Plots of the simulation results are located in Figure 4-2. First the defect introduction rate was determined to be 1.47 x 10^4 Vacancies/Ion/cm. The normalized V_{oc} results of 0.91 and 0.67 produced by the model at fluences of 1×10^{12} protons/cm^2 and 1×10^{14} protons/cm^2, respectively, compare well with those of Jasenek et al. [55]. The larger percentage difference between experimental and modeled results for the open-circuit voltage at a fluence of 1×10^{12} protons/cm^2 can probably be attributed to the diode idealty factor, A, being slightly small and the initial defect density being slightly too large. Again, the values for the normalized I_{sc} are better, as compared to the experimental results of Jasenek et al. [55], at a fluence of 1×10^{12} protons/cm^2 with a value of 1.0, while there is a much greater difference produced at a fluence of 1×10^{14} protons/cm^2 with a result of 0.75. One possibility for the great difference in the short-circuit value is the exponential curve that was used to model it and will be discussed further in section 4.3. Another possibility is that the value of α may not have been high enough. In equation 7, the value of α equal to 0.9×10^{-16} A/proton and the value of γ_c used in equation 12 was 1050 cm^{-1}. Next, the values produced by the model for the normalized fill-factor at fluences of 1×10^{12} protons/cm^2 and 1×10^{14} protons/cm^2 are 0.99 and 0.91, respectively. These results are slightly higher than the experimental results but still compare well with experimental results produced by Jasenek et al. [55]. The values produced by the model for the normalized efficiency are 0.89 and 0.45 at fluences of 1×10^{12} protons/cm^2 and 1×10^{14} protons/cm^2, respectively. While the simulation results are lower than the experimental values of the normalized efficiency, it can be seen that there is a good

match between the two sets of data. Differences between the experimental and modeled results for the efficiency are probably due to differences in the open-circuit voltage and the short-circuit current. As can be seen from the tables and figure below, 1 MeV protons still cause a large amount of damage to the efficiency, but do not cause near as much as the 290 keV protons.

Table 4.5 – *Experimental Results from Jasenek et al. [55] for 1MeV protons.*

Fluence	Norm. V_{oc}	Norm. I_{sc}	Norm. FF	Norm. Efficiency
1×10^{12}	0.98	0.97	0.99	0.95
1×10^{14}	0.68	0.63	0.91	0.47

Table 4.6 – *Simulation results for 1 MeV protons.*

Fluence	Norm. V_{oc}	Norm. I_{sc}	Norm. FF	Norm. Efficiency
1×10^{12}	0.91	1.0	0.99	0.89
1×10^{14}	0.67	0.75	0.91	0.45

Table 4.7 - *Percentage difference between Jasenek et al. [55] and simulation results*

for 1 MeV protons.

Fluence	Norm V_{oc}	Norm. I_{sc}	Norm. FF	Norm. Efficiency
1×10^{12}	7.14%	-3.09%	0%	6.32%
1×10^{14}	1.47%	-19.05%	0%	4.26%
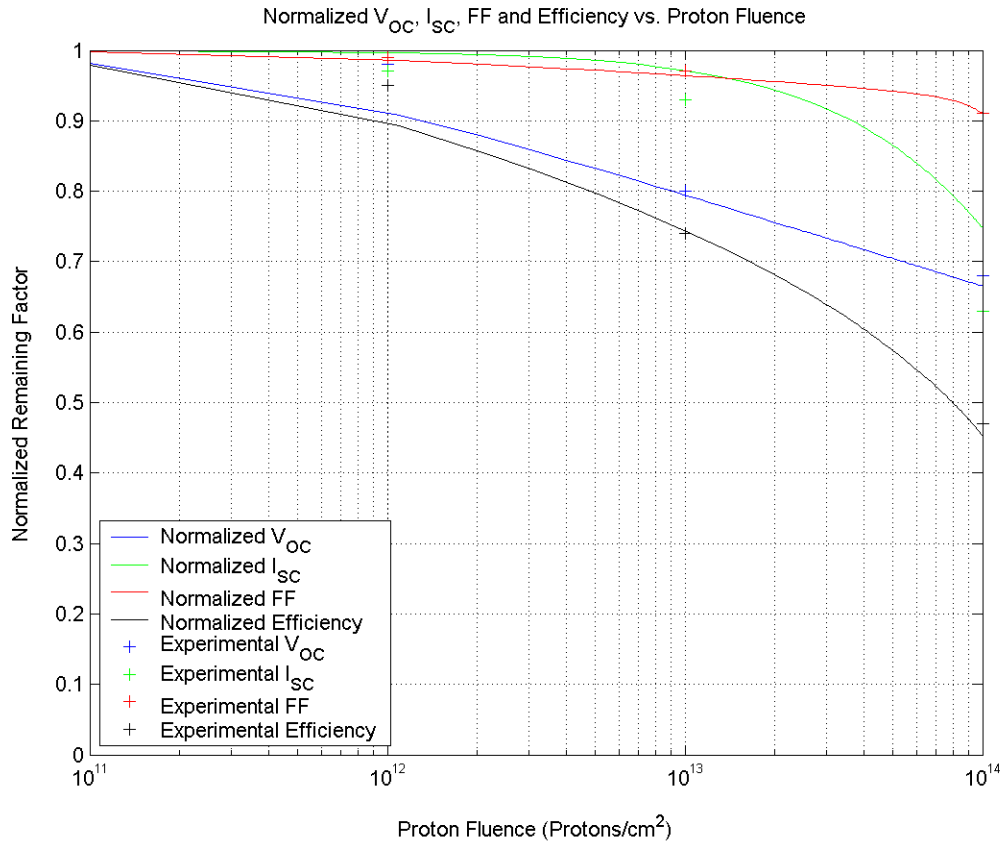
Figure 4-2 - - Normalized open-circuit voltage, short-circuit current, fill-factor, and efficiency for 1 MeV proton irradiation. Experimental results are those of Jasenek et al. [55].

The last results are that of the 10 MeV protons. Results from both experiment, conducted by Jasenek et al. [55], simulation, and percentage difference between the experimental and simulation results for 10 MeV proton irradiation are presented in Tables 4.8, 4.9, and 4.10, respectively. In addition, plots produced from the simulation results are presented in Figure 4-3. First, the defect introduction rate was determined to be 1.98 x 10^3 Vacancies/Ion/cm. Values produced by the CIGS Calculator model for the normalized V_{oc} are 0.98 and 0.78 for fluences of $1x10^{12}$ protons/cm^2 and $1x10^{14}$ protons/cm^2, respectively. As seen, these values compare well with the experimental results of Jasenek et al. [55]. Again this could partially be due to the diode ideality factor, A, and the initial defect density being too large. In order to produce a match to the experimental results of Jasenek et al. [55], the value of α used in equation 7 was $0.3x10^{-16}$ A/proton which produced values for the normalized short-circuit current of 1.0 and 0.91 for fluences of $1x10^{12}$ protons/cm^2 and $1x10^{14}$ protons/cm^2, respectively. The value of γ_c used in equation 12 was 0 cm^{-1}. Next, the values for the fill-factor produced by the model at fluences of $1x10^{12}$ protons/cm^2 and $1x10^{14}$ protons/cm^2 were 1.0 and 0.96, respectively, which are elevated compared to the results produced by Jasenek et al. [55]. Raised values for the fill-factor are probably due to the calculation of the series resistance. There could be several things causing this. One could be poor values for the hole and electron mobilities as general values were used here. Second, the value for the initial acceptor level could be off as this was taken from the modeling effort of Gloeckler et al. [25]. The third, and probably the largest contributing factor is the value for the introduction rate for compensating defects could be too small. Raising γ_c would cause the acceptor density to decrease thus causing the resistivity and series

resistance to increase and thus lowering the fill-factor. The values produced by the model for the normalized efficiency were 0.97 and 0.68 at fluences of 1×10^{12} protons/cm^2 and 1×10^{14} protons/cm^2 which agrees well with experimental results produced by Jasenek et al. [55]. The slightly high difference between experimental results and those of the model at a fluence of 1×10^{14} protons/cm^2 is attributed to differences in the open-circuit voltage, short-circuit current and fill-factor. It should be noted that 10 MeV protons cause less damage to the efficiency than both the 290 keV and 1 MeV protons.

Table 4.8 – *Experimental Results from Jasenek et al. [55] for 10MeV protons.*

Fluence	Norm. V_{oc}	Norm. I_{sc}	Norm. FF	Norm. Efficiency
1×10^{12}	0.98	0.99	0.97	0.98
1×10^{14}	0.79	0.90	0.91	0.65

Table 4.9 – *Simulation results for 10MeV protons.*

Fluence	Norm. V_{oc}	Norm. I_{sc}	Norm. FF	Norm. Efficiency
1×10^{12}	0.98	1.0	1.0	0.97
1×10^{14}	0.78	0.91	0.96	0.68

Table 4.10 - *Percentage difference between Jasenek et al. [55] and simulation results*

for 10 MeV protons.

| Fluence	Norm. V_{oc}	Norm. I_{sc}	Norm. FF	Norm. Efficiency
1×10^{12}	0%	-1.01%	-3.09%	1.02%
1×10^{14}	-1.28%	-1.11%	-5.49%	4.62%
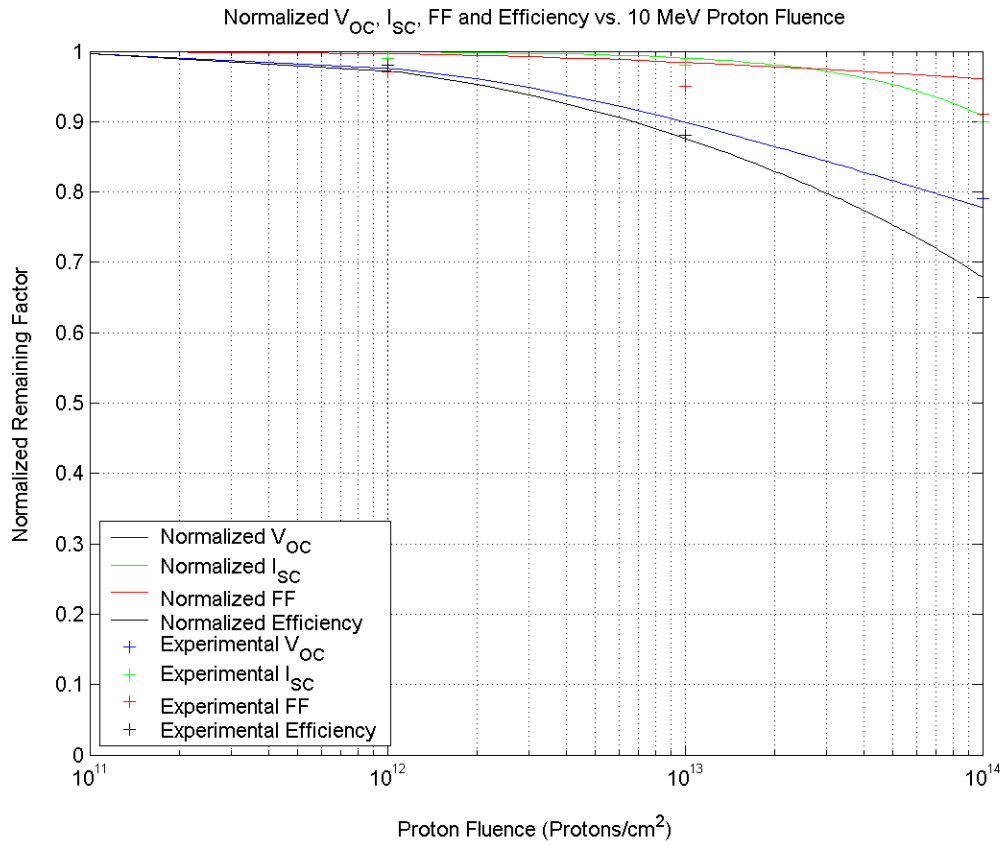
Figure 4-3 - Normalized open-circuit voltage, short-circuit current, fill-factor, and efficiency for 10 MeV proton irradiation. Experimental results are those of Jasenek et al. [55].

4.2   Simulation II

In this section, simulations were completed and compared to the experimental

results of Boden et al. [49]. Simulations were run at proton energies of 100 keV, 500

keV, 1 MeV, and 3 MeV. It should be noted that the illumination spectrum used by

Boden et al. [49] to obtain their results was not provided. A fluence of

9.99×10^{4} protons/μm^{2}, which is equivalent to 9.99×10^{12} protons/cm^{2}, was used in the

simulation. It should also be noted that the simulation results are actually at a fluence of

3.10×10^{12} rather than 3.0×10^{12}. This small difference is considered to be negligible for

comparison of the results produced by the simulation and those produced experimentally

by Boden et al. [49]. Table 4.11 details the structure and layer thicknesses that were used

for the simulation. The only layer where any real information was given was for the

CIGS layer and that the other layers did exist [49]. For the thickness of the CdS, ZnO,

and Al doped ZnO layers, information from Jasenek et al. [55] was used. Initial values

for V_{oc} and I_{sc} were not given; therefore initial values from Jasenek et al. [55] were used.

Table 4.11 – *Structure used to simulate results of Boden et al. [49].*

Layer Name	Thickness (Angstroms)
ZnO –doped with Al	3000
ZnO	500
CdS	500
CIGS	1.6 μm

Information for the experimental results of Boden et al.[49], simulation results

and the percentage difference between the two sets of results for 100 keV proton

51

irradiation are detailed in Tables 4.12, 4.13, and 4.14. Plots of all results can be seen in

Figure 4-4. Boden et al. [49] only provided results for all solar cell parameters after a

proton fluence of $3x10^{12}$ protons/cm^2. The defect introduction rate calculated was

$1.25x10^4$ Vacancies/Ion/cm. Data obtained by the simulation for the normalized V_{oc} is

0.87 which is considerably lower than the value obtained by Boden et al. [49]. One

possible reason for this is that the diode ideality factor is too small. Another possible

reason is that the initial defect density was too large. The value for α used in equation 7

is $0.811x10^{-16}$ A/proton and the value of γ_c used in equation 12 was 947.2 cm^{-1}. Values

for the normalized I_{sc} and FF are very close to those obtained experimentally by Boden et

al. [49]. Results for the normalized efficiency were quite different than those obtained

experimentally by Boden et al. [49] which is partially attributed to the difference in the

calculation of V_{oc}. It should be noted that 100 keV protons cause more damage to the

efficiency than the 10MeV protons and less damage than the 290 keV and 1 MeV protons

from the previous simulations. One note that should be taken into account when

comparing the results of the two simulation sets is that the thickness of the CIGS layer is

different which will cause the defect introduction rate and thus the modeling results to be

different.

Table 4.12 – *Experimental Results from Boden et al. [49] for 100 keV protons.*

Fluence	Norm. V_{oc}	Norm. I_{sc}	Norm. FF	Norm. Efficiency
$3x10^{12}$	0.99	0.99	0.97	0.96

Table 4.13 – *Simulation results for 100 keV protons.*

Fluence	Norm. V_{oc}	Norm. I_{sc}	Norm. FF	Norm. Efficiency
3×10^{12}	0.87	0.99	0.98	0.84

Table 4.14- *Percentage difference between Boden et al. [49] and simulation results*

for 100 keV protons.

Fluence	Norm. V_{oc}	Norm. I_{sc}	Norm. FF	Norm. Efficiency
3×10^{12}	12.12%	0.0%	-1.03%	12.5%

Simulations for 500 keV protons were the next to be completed. Results for the experimental results of Boden et al. [49], simulation results, and the percentage difference between the two sets of results are shown in Tables 4.15, 4.16, and 4.17, and plotted in Figure 4-5. The defect introduction rate used was 2.85×10^4 Vacancies/Ion/cm. Simulation results obtained for the normalized V_{oc} agree well with those obtained experimentally by Boden et al. [49]. The small percentage difference between the two sets of results could be attributed to the diode ideality factor, A, being slightly too large. The value of α used for equation 7 to calculate the current is 1.406×10^{-16} A/proton and the value of γ_c used in equation 12 was 1509 cm^{-1}. Normalized short-circuit current, FF, and efficiency values obtained by the simulation are considerably higher than those of Boden et al. [49]. There are two possibilities for the abnormal results of the short-circuit current. First, the value for α might be too low causing the current value to be too high. Second, is that when modeling the current, an exponential curve was used whereas a slightly different curve may have produced a better result. This will be discussed more in

section 4.3. Abnormally high values for the normalized FF and efficiency are most likely due to the abnormally high values obtained for I_{sc} and the slightly large value of V_{oc}. Another possible reason for the abnormally high values of the FF could be due to the fact that the series resistance may not be high enough which can be caused by γ_c not being high enough causing the series resistance to be too small. It should be noted that the 500 keV protons cause considerably more damage to the efficiency than did the 100 keV protons.

Table 4.15 – *Experimental Results from Boden et al. [49] for 500 keV protons.*

Fluence	Norm. V_{oc}	Norm. I_{sc}	Norm. FF	Norm. Efficiency
$3x10^{12}$	0.75	0.92	0.83	0.57

Table 4.16 – *Simulation results for 500 keV protons.*

Fluence	Norm. V_{oc}	Norm. I_{sc}	Norm. FF	Norm. Efficiency
$3x10^{12}$	0.77	0.99	0.96	0.73

Table 4.17 - *Percentage difference between Boden et al. [49] and simulation results for 500 keV protons.*

| Fluence	Norm. V_{oc}	Norm. I_{sc}	Norm. FF	Norm. Efficiency
$3x10^{12}$	-2.67%	-7.61%	-15.66%	-28.07
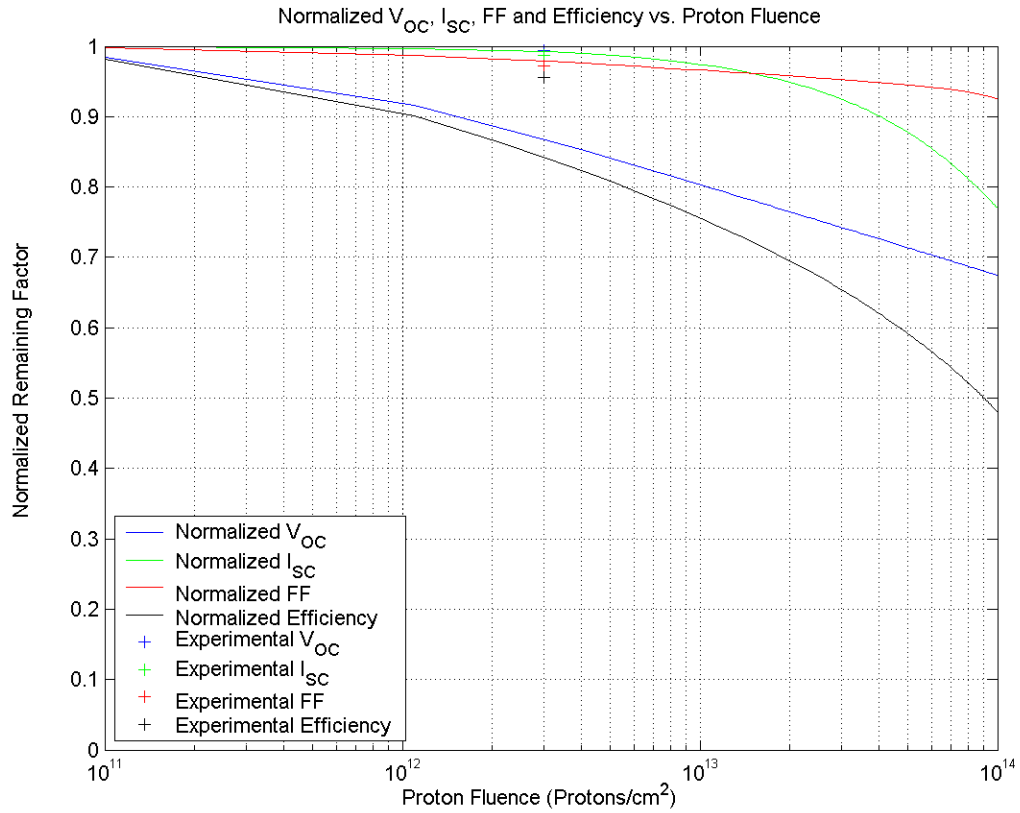
Figure 4-4 - Normalized open-circuit voltage, short-circuit current, fill-factor, and efficiency for 100 keV proton irradiation. Experimental results are those of Boden et al. [49].
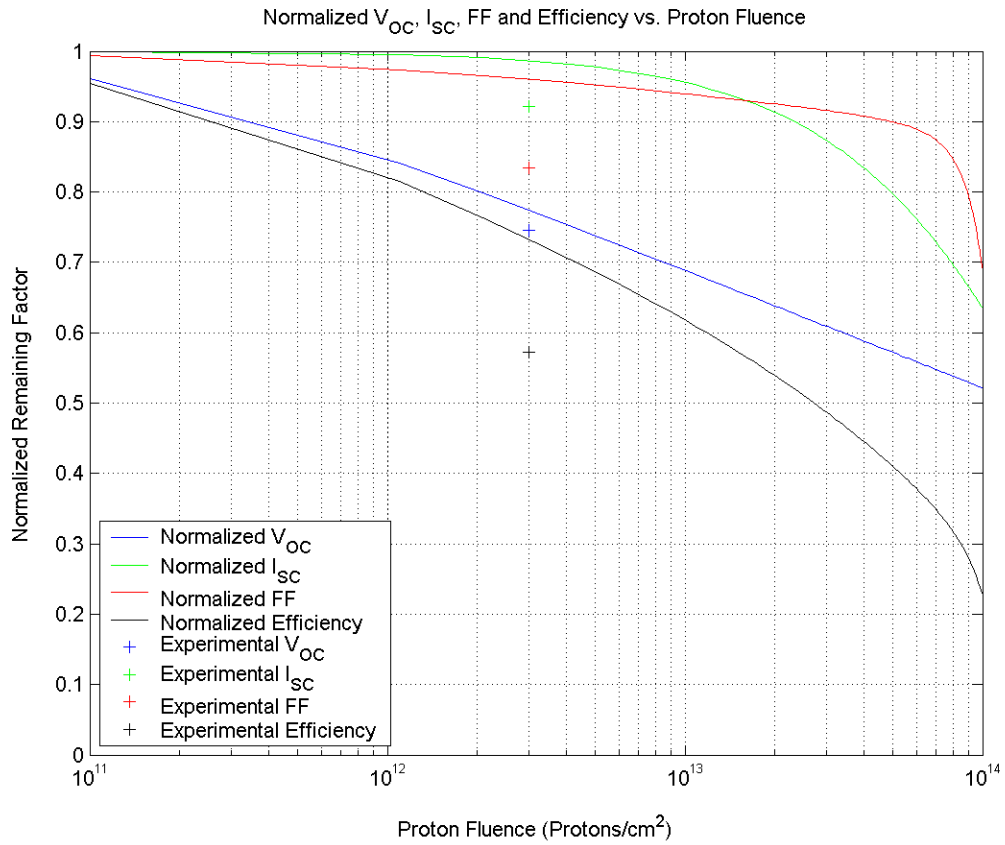
Figure 4-5 - Normalized open-circuit voltage, short-circuit current, fill-factor, and efficiency for 500 keV proton irradiation. Experimental results are those of Boden et al. [49].

Experimental results of Boden et al. [49], simulation results and percentage difference calculations between the two for 1 MeV protons are presented in Tables 4.18, 4.19, 4.20 and Figure 4-6. The defect introduction rate used was 1.53×10^4 Vacancies/Ion/cm. At a fluence of 3×10^{12} protons/cm^2, the normalized V_{oc} compared well with Boden et al. [49] and the simulation producing results of 0.88 and 0.86 respectively. The value of α used in equation 7 to calculate the current was 0.924×10^{-16} A/proton and the value of γ_c used in equation 12 was 1076 cm^{-1}. Values of I_{sc} and efficiency obtained by the simulation all agreed relatively well with the experimental results of Boden et al. [49]. One exception is the fill-factor value obtained from the simulation which is slightly high. This could be partially explained by the differences in the open-circuit voltage and short-circuit current results. Another reason could be that the series resistance could be too low which could be caused by γ_c being slightly too small. It can be seen that 1 MeV protons cause more damage to the efficiency than the 100 keV protons and less than the 500 keV protons.

Table 4.18 – *Experimental Results from Boden et al. [49] for 1MeV protons.*

Fluence	Norm. V_{oc}	Norm. I_{sc}	Norm. FF	Norm. Efficiency
3×10^{12}	0.88	0.98	0.94	0.81

Table 4.19 – *Simulation results for 1MeV protons.*

Fluence	Norm. V_{oc}	Norm. I_{sc}	Norm. FF	Norm. Efficiency
3×10^{12}	0.86	0.99	0.98	0.83

Table 4.20 - *Percentage difference between Boden et al. [49] and simulation results*

for 1 MeV protons.

Fluence	Norm. V_{oc}	Norm. I_{sc}	Norm. FF	Norm. Efficiency
$3x10^{12}$	2.27%	-1.02%	-4.26%	-2.47%
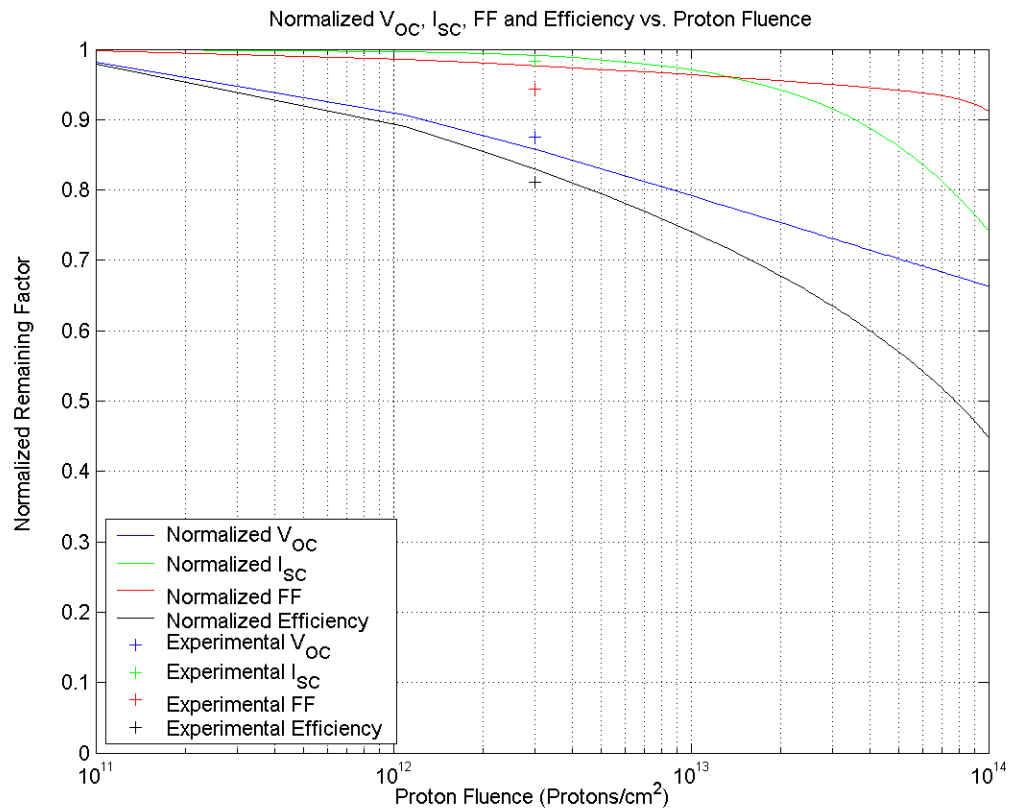
Figure 4-6 - Normalized open-circuit voltage, short-circuit current, fill-factor, and efficiency for 1 MeV proton irradiation. Experimental results are those of Boden et al. [49].

Simulations for 3 MeV were next to be completed. Experimental results obtained

by Boden et al. [49], simulation results and the percentage difference between the two

different sets of results are detailed in Tables 4.21, 4.22, 4.23 and in Figure 4-7. The

defect introduction rate obtained was 5.42×10^3 Vacancies/Ion/cm. Values obtained for

the normalized V_{oc} at a fluence of 3×10^{12} protons/cm^2 were 0.93 and 0.91 for the

experimental results obtained by Boden et al. [49] and the simulation, respectively. The

value of α obtained for use in equation 7 was 0.491×10^{-16} A/proton and the value of γ_c

obtained for use in equation 12 was 470.8 cm^{-1}. The results of the simulation agree well

with the results of Boden et al. [49] for the I_{sc} and efficiency as can be seen in the tables

below. The fill-factor has a slightly higher percentage difference than should be present.

This could easily be attributed to two different reasons. First, the difference could be due

to differences between the values calculated by the model and values found

experimentally for the open-circuit voltage and short-circuit current. Second, the series

resistance value that was calculated could be slightly too small. A small value for the

series resistance is most likely caused by γ_c being too small. It can be seen that the 3 Mev

protons cause less damage to the efficiency than the 500 keV and 1 MeV protons while

they cause more damage than the 100 keV protons.

Table 4.21 – *Experimental Results from Boden et al. [49] for 3 MeV protons.*

Fluence	Norm. V_{oc}	Norm. I_{sc}	Norm. FF	Norm. Efficiency
3×10^{12}	0.93	0.99	0.96	0.88

Table 4.22– *Simulation results for 3MeV protons.*

Fluence	Norm. V_{oc}	Norm. I_{sc}	Norm. FF	Norm. Efficiency
$3x10^{12}$	0.91	1.0	0.99	0.89

Table 4.23 - *Percentage difference between Boden et al. [49] and simulation results*

for 3 MeV protons.

| Fluence	Norm. V_{oc}	Norm. I_{sc}	Norm. FF	Norm. Efficiency
$3x10^{12}$	2.15%	-1.01%	-3.13%	-1.14%
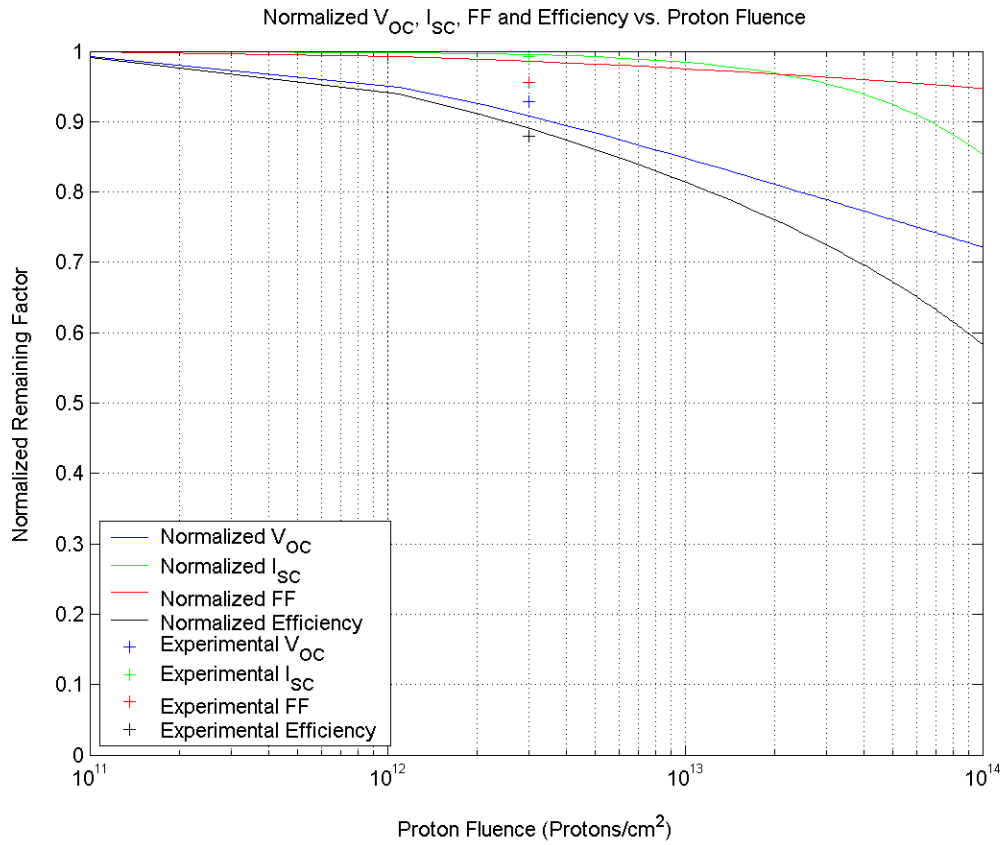
Figure 4-7 - Normalized open-circuit voltage, short-circuit current, fill-factor, and efficiency for 3 MeV proton irradiation. Experimental results are those of Boden et al. [49].

4.3   Discussion

When developing the model, there were several equations available to solve for all quantities. One of the most challenging items to model was the fill-factor and efficiency. Values that were obtained were often much higher than those obtained experimentally by Jasenek et al. [55]. The problem was determined to come from the calculation of the series resistance. To fix the problem, the change in the acceptor concentration N_A with proton irradiation needed to be taken into account as described in the previous chapter.

Another major challenge was to properly model the short-circuit current. Several different equations were attempted, but the results were still extremely different from experimental results. A curve was then fitted to the current data in Jasenek et al. [55] where an exponential curve was used as can be seen in equation 7 in chapter 3. One issue is that the curve seems to provide results that are larger than the experimental results at fluences around the 1×10^{13} protons/cm^2. One possibility to fix this is to use a different curve, such as the polynomial curve that was used to find values for α and γ_c.

The results of the model produced several results that showed considerable differences and were not limited to results of a particular energy proton or specific parameter such as the open-circuit voltage or fill-factor. In the following, reasons for differences in the calculation of each parameter are presented. For open-circuit voltage calculations, the largest contributing sources of differences are believed to be the diode ideality factor, A, and the number of initial defects in the material. Small changes in either of these can cause large changes in the open-circuit voltage value. Another source of differences was the value α used for calculating the short circuit current. If the value

63

of α was too large, the short-circuit current would be too small and too large if α was too

small. There were two main reasons why the fill-factor would be extremely different

from experimental results. First, the series resistance could be too high or too low. This

can be caused by the introduction rate of compensating defects, γ_c, being too small. If γ_c

is too small, then the acceptor density is too large. When the acceptor density is too

large, the resistivity and series resistance are too small. The second reason is that if the

open-circuit voltage and short-circuit current values have large differences in the

calculated values, that difference carries into the fill-factor calculation. The third, and

probably the least contribution to the differences, is the band gap energy, initial acceptor

concentration, hole mobility, and electron mobility values. Though the band-gap energy

can be computed, the information required is not always available. Also, values for the

initial acceptor concentration are general values and are not from data for a specific

sample. The mobility values that are used are general values and are not actual values at

a given temperature and doping level like one would find for silicon or GaAs.

Differences in the efficiency calculation can be largely attributed to a summation of

everything that has been discussed to this point as the calculation of the efficiency relies

on values calculated for the open-circuit voltage, short-circuit current and fill-factor.

Boden et al. [49] did not provide the test conditions that were used. If testing was

completed using AM0 spectrum and the model uses an AM1.5 spectrum, the results can

be incorrect for the calculation of the efficiency. Another possible source of differences

is the accuracy of the proton irradiation of Boden et al. [49]. Inaccuracies in the proton

irradiation could mean that the result obtained for a given fluence, is really the result for a

slightly different fluence. Another point is that Kroon et al. [50] found differences

between the results of Boden et al. [49] and results produced by SRIM. It should be noted that Kroon et al. [50] used damage coefficients for comparing results and did not look at a particular parameter at a given fluence as this model has done. For purposes of this model, this explanation would only be pertinent for the 100 keV proton simulations as Kroon et al. [50] found that the SRIM and experimental results of Boden et al. [49] matched well from 500 keV to 3 MeV. The next possible source of differences was the lack of initial cell parameters provided by Boden et al. [49]. Results produced by this model are dependant on initial values. For example, if there is a 20 mV drop in the open-circuit voltage, the remaining factor will be larger and smaller for smaller and larger initial values of the open-circuit voltage. One last source of difference is that general values for the composition of the CIGS material were used [JEG]. Variations in the composition could make some differences in the modeling results.

There are three main results that can be derived from the results shown that confirm previous results. First, the lower the energy of the incident proton, more vacancies are created within the sample. For example, 290 and 500 keV protons cause significantly more damage than 1, 3, and 10 MeV protons. One exception is that low energy particles with energies in the 100 – 200 keV range cause less damage than the 290 and 500 keV protons as many of the protons are stopped before entering the absorber layer. Second, the more protons that are incident on the sample, the lower the acceptor concentration N_A is causing a larger series resistance and even lower FF and η. Third, the more vacancies that are created within the material, the more cell parameters such as V_{oc}, I_{sc}, FF, and η are degraded. Using this information, one can calculate the approximate EOL values for basic cell parameters.

CHAPTER 5 CONCLUSION

Radiation causes much damage to solar cells being used in space. Many times, lengthy experiments must be conducted to determine the damage caused to a solar cell. Using this model requires very few inputs as compared to other modeling programs that are presently being used and requires only basic testing of the sample solar cell to obtain the open-circuit voltage and short-circuit current. This model also allows for a great amount of freedom and flexibility to study new materials, CIGS layer compositions, and cell coatings easily whereas with other models, this cannot be completed as readily. With a small amount of information and testing this model provides the actual and normalized remaining factors of the open-circuit voltage, short-circuit current, fill-factor and efficiency that were only previously available with long and lengthy experimentation and modeling.

5.1   Lessons Learned

Through the creation and use of this model, several things have been learned. It should also be noted that the results of the project confirm previous results. First, is the lower the proton energy, the more vacancies are created within the material as the ion does not pass through the solar cell. The only exceptions to this are protons in the range of 100-200 keV, as they are low enough energy that most of the vacancies are caused before reaching the absorber layer. Another point is that the more vacancies that are created, the acceptor concentration decreases due to compensating defects that are created. This causes the series resistance within the absorber to increase which causes the fill-factor and efficiency to decrease. Third, the more vacancies that are created within the material, the more cell parameters such as V_{oc}, I_{sc}, FF, and η are degraded.

66

Using this information, one can calculate the approximate EOL values for basic cell parameters.

5.2   Modeling Results

Though the majority of calculations made by the model were accurate, there are still several differences that occurred. There was no pattern to differences with regards to different proton energies. The largest differences seemed to occur around fluences of 10^{13} protons/cm^2. For current calculations, this was evident in simulation I results for 290 keV and 1 Mev protons. A possible reason for this could have been the model used for the current. A polynomial or other more linear fit such as used for α and γ_c may have been more appropriate by providing more of a slope, in that region of the curve. Results for the open-circuit voltage produced differences with respect to experimental results with proton fluences of 10^{13} cm^{-2}. Precise reasons for the differences are not known. Differences produced for the fill-factor are believed to be from a combination of differences in the open-circuit voltage and short-circuit current as well as differences in the calculation of the series resistance. Considerations in the calculation of the series resistance will be discussed shortly. Problems with efficiency calculations at this fluence are believed to be the effect of differences in all other calculations.

In general, there are many possible reasons for differences produced by the model. For the open-circuit voltage there were two factors possibly contributing to the differences. First, the diode ideality factor could be off as previously mentioned. Also, the diode ideality factor is set as a single number throughout the model. It should be changing as does the open-circuit voltage and short-circuit current. Differences produced for short-circuit current results are thought to be caused by two reasons. One is the

67

values of α that is used which affect the decay of the exponent in equation 7. The second is that a more linear model should be used to model the current as previously discussed. Calculation differences produced by the model for the fill-factor can be attributed to two main factors. First, are differences produced in the calculation of the open-circuit voltage and short-circuit current. Second, are differences in the calculation of the series resistance. This is believed to be primarily caused by a difference in the value of γ_c, the introduction rate of compensating defects. When γ_c is too small, then the acceptor density is calculated to be larger than it should be. When the acceptor density is too large, then the resistivity and the series resistance are too small. Other sources of differences are because the values for the band-gap energy and initial acceptor concentration that come from literature and are not specific to a specific model. Though differences in the electron and hole mobilities, initial acceptor concentration, and band-gap energy can play a role in differences produced in the calculation of the series resistance, it is thought to have a minimal effect. Differences produced in the calculation of the efficiency are believed to result from differences in the calculation of the open-circuit voltage, short-circuit current and fill-factor. Also, Boden et al. [49] did not state whether testing was completed under AM 0 or AM 1.5 illumination which will produce differences in the calculation of the efficiency if the wrong values are used. Another possible source of differences is the accuracy of the fluence used by Boden et al [49]. Inaccuracies in the proton irradiation could mean that the result obtained for a given fluence, is really the result for a slightly different fluence. One last point is that Kroon et al. [50] found differences between the results of Boden et al. [49] and results produced by SRIM. It should be noted that Kroon et al. [50] used damage coefficients for comparing

results and did not look at a particular parameter at a given fluence as this model has

done. For purposes of this model, this explanation would only be pertinent for the 100

keV proton simulations as Kroon et al. [50] found that the SRIM and experimental results

of Boden et al. [49] matched well from 500 keV to 3 MeV. Another possible problem is

the lack of initial values provided by Boden et al. [49]. The model relies on initial values

to calculate the remaining factor of the cell parameters and the lack of this information

can produce differences in the calculations. One last possible source of differences is that

general values were used for the composition of the CIGS material. Variations in the

composition of the CIGS material could cause some differences in the results of the

model.

5.3   Future Revisions

The most important enhancement that could be made to the program is to

incorporate the constants α, introduction rate of compensating defects, γ_c, and the diode

ideality factor better. For the constants α and γ_c, the best course of action would be to

acquire more data from experiments and produce a fit of these variables to said data.

This would provide a more accurate model of how these constants change with respect to

the defect introduction rate. As for the diode ideality factor, A, an educated guess is

used. Also, the same value of A is used for all calculations, regardless of proton fluence,

which is incorrect as the open-circuit voltage and short-circuit current change after a

given proton fluence. As the ideality factor is linked to the I-V characteristics as

explained in Green [2], it would be good to recalculate A for every calculations

performed for each fluence value. The obstacle is that the voltage and current must be

calculated prior to calculating A, thus causing the problem of too many unknowns. There

could be ways to remedy this problem though, which would help to provide even more accurate results.

In order to make the model as realistic as possible, it would be beneficial to allow other elements such as atomic oxygen as well as different particle energies to be simulated together [9]. In order to do this, the DataBuilder program must be updated to allow for users to input this information and to ensure that the maximum number of ions that SRIM can handle at once has not been exceeded.

Another revision for the future would be to consolidate all of the functions that are now completed by different software packages. It would be very beneficial if a standard MS Windows based program were to be created that included a better user interface, as well as encompassed all of the functionality of SRIM, Excel, MATLAB, and Mathcad. Mathcad and MATLAB functionality could be included by using a plug-in with graphing capability.

APPENDIX A – DATABUILDER C++ CODE

Driver.cpp

```cpp
//Jacob Dunken
//DataBuilder - Master
//Driver.cpp

#include <iostream> //for cout, etc.
using namespace std;
#include "DB.h"

int main()
{

    cout << "DataBuilder\nJacob Dunken\n\n\n";

    DB data; //create instance of DB class
    data.Write(); //call Write function

    return 0;
}
```

DB.h

```cpp
//Jacob Dunken
//DB.h

#ifndef _DBH_H //if its not defined, define it
#define _DBH_H

#pragma warning(disable: 4786)
#include <vector>  //use for vectors

using namespace std;

class DB
{
private:
      void FillPos();
      void FillAngle();

      vector<int> position;
      vector<double> angle;
      int NumIons, xposition, energy, ion, RandNum;

public:
      DB();
      void Write();

};
#endif
```

DB.cpp

```cpp
//Jacob Dunken
//DB.cpp

#pragma warning(disable:  4786)
#include<fstream> //for file IO
#include<algorithm> //for random shuffle alg.
#include<iomanip> //for formatting
#include<vector> //for vectors
#include<cmath> //math functions, cos, etc
#include<iostream> //IO control
using namespace std;
#include "DB.h"

DB::DB()
{
      //fill position vector
      FillPos();

      //Fill angle vector
      FillAngle();

      //set postion in x direction to 0
      xposition = 0;
}
void DB::FillPos()
{
      //Fill Position Vector

      int x = -5000; //Starting point
      for(int i = 0;i < 10002; i++)
      {
            position.push_back(x);
            x++;
      }
}
void DB::FillAngle()
{
      //Fill Angle Vector

      int x = 0; //Starting Point
      for(int i = 0;i<181;i++)
      {
            angle.push_back(cos(x * (3.14159 / 180.0)));
            x++;
      }
}
//Write Data to File
void DB::Write()
{
      //Create output file and get filename
      ofstream output;
```

```cpp
    char filename[52] = "trim.dat";
    output.open(filename, ios::out);

    //make sure file is created and open
    if (!output)
    {
        //if no file - put to screen
        cout << "no file";
    }
    else
    {
        //Init. vars. for user input.
        char date[52], line1[100], line2[100], line3[100];
        char stoich[100];

        //Write header to file
        output << "Jacob Dunken\n";

        //Collect information from user
        cout << "\nEnter the number of ions to be simulated>>";
        cin >> NumIons;

        cout << "\nEnter a seed value for the random number" <<
                " generator>>";
        cin >> RandNum;

        cin.ignore();

        cout << "\nEnter Date of creation>>";
        cin.getline(date,50);
        output << "Date:  " << date << "\n";

        cout << "\nEnter the ion energy>>";
        cin >> energy;

        cout << "\nEnter atomic number of ion>>";
        cin >> ion;
        cin.ignore();

        cout << "\nEnter comments line 1>>";
        cin.getline(line1,100);

        cout << "\nEnter comments line 2>>";
        cin.getline(line2,100);

        cout << "\nEnter comments line 3>>";
        cin.getline(line3,100);

        cout << "\nEnter coumpound including stoichiometry>>";
        cin.getline(stoich,100);

        //Write information to file
        output << "The atomic number of the ion is >>" <<
                ion << "\n";
        output << line1 << "\n";
```

```cpp
output << line2 << "\n";
output << line3 << "\n";

//Format - align text to left
output.setf(ios::left);

//Write Column Headers to File
output << endl << setw(10) << "Event #" <<
      setw(10) << "Atom #" << setw(10) <<
      "Energy(eV)" <<
      setw(10) << "X(Ang)" << setw(10) <<
      "Y(Ang)" << setw(10) << "Z(Ang)" <<
      setw(10) << "Cos(X)" << setw(10) <<
      "Cos(Y)" << setw(10) << "Cos(Z)\n";

//Undo left align
output.setf(ios::left);

//Put separation between header and data
output << "_____" <<
      "_____\n";

//Format numbers
output.setf(ios::showpoint);
output.setf(ios::fixed);
output.precision(4);

//Start creating and writing data to file

//initiate counter
int count = 0;
for(int i = 0; i < NumIons; i++)
{

      //shuffle vectors every 5 iterations
      if(count == 5)
      {
        random_shuffle(angle.begin(), angle.end());
        random_shuffle(position.begin(),position.end());
            count = 0;
      }

      //seed the random number generator
      srand(RandNum);

      //format numbers
      output.setf(ios::fixed);
      output.setf(ios::showpoint);
      output.precision(4);
      output.setf(ios::left);

      //write data to file
      output << setw(10) << i << setw(10) <<
            ion << setw(10) <<
            energy << setw(10) << xposition <<
```

76

```cpp
                    setw(10) << position.at(rand()%10000) <<
                    setw(10) << position.at(rand()%10000) <<
                    setw(10) << angle.at(rand()%180) <<
                    setw(10) << angle.at(rand()%180) <<
                    setw(10) << angle.at(rand()%180) << "\n";

            //increment random number seed value and count values
            RandNum++;
            count++;
        }
        //close output file
        output.close();
    }
}
```

APPENDIX B – CIGS CALCULATOR C++ CODE

Driver.cpp

```cpp
//Jacob Dunken
//CIGS Calcs
//Thesis Project

//Driver.cpp

#include "calculator.h"
#include "fluence.h"


int main()
{
    //Create Instance of Calculator Class
    Calculator CIGS;

    return 0;
}
```

Calculator.h

```cpp
//Jacob Dunken
//CIGS Calcs
//Thesis Project

//calculator.h

#ifndef _CALCULATOR_H //if it is isn't defined, define it..
#define _CALCULATOR_H

#include <fstream>
using namespace std;

class Calculator
{
private:
      void printHeader();
      void getInitial();
      void doCalcs();
      void openOut();
      ofstream out;
public:
      Calculator();
      double defIntRate, begFluence, endFluence, dataPoints;

};
#endif
```

Calclator.cpp

```cpp
//Jacob Dunken
//CIGS Calcs
//Thesis Project

//calculator.cpp

#include <iostream> //IO control
#include <fstream> //file output
#include <string> //for use of strings
#include <iomanip> //IO format
using namespace std;
#include "calculator.h"
#include "fluence.h"

Calculator::Calculator()
{
     printHeader(); //print header to screen
     getInitial(); // Get values from user
     openOut(); //setup output file
     doCalcs(); //perform all calcs.
}

//Print Header to Screen
void Calculator::printHeader()
{
     cout << "CIGS Calculator\n\\Jacob Dunken\nThesis Project";
}
//Get Initial data from user.
void Calculator::getInitial()
{
     cout << "\n\nEnter Calculated defect introduction rate>>";
     cin >> defIntRate;
     cin.ignore();
     cout << "\n\nEnter beginning fluence>>";
     cin >> begFluence;
     cin.ignore();
     cout << "\n\nEnter ending fluence>>";
     cin >> endFluence;
     cin.ignore();
     cout << "\n\nEnter number of data points>>";
     cin >> dataPoints;
     cin.ignore();
}
void Calculator::openOut()
{
     //Get filename for output file
     string filename;
     cout << endl << "Please enter output filename" <<
             " (include extionsion) >>";
     getline(cin,filename);
```

```cpp
            //open output file
            out.open(filename.c_str(), ios::out);
            if (!out)
            {
                    //if can't open send message and return false
                    cout << endl << "NO FILE";
            }
            else
            {
                    //Write Header to Output file
                    out << "CIGS Calculator\nJacob Dunken\n\n\n";


                    out.setf(ios::left); //have text go to left

                    //Write Column Headers
                    out << setw(12) << "PHI" << setw(10) <<
                            "Voc" << setw(10)<< "NVoc" << setw(10) <<
                            "current" << setw(10) << "NormI" <<
                            setw(10) <<  "Vmp" << setw(10) << "Imp" <<
                            setw(10) << "FF" << setw(10) << "NFF" <<
                            setw(10) << "Efficiency" << setw(10) <<
                            "Nefficiency" << endl;

                    //Take off left format
                    out.unsetf(ios::left);
            }
    }

    void Calculator::doCalcs()
    {
            Fluence sample; //Create Fluence Object

            //Set Initial Phi
            sample.setPhi(0.00);

            //Set Defect Int. Rate
            sample.setDefRate(defIntRate);

            //Call function to make calcs. for Phi = 0
            sample.runCalcs();

            //Format numbers
            out.setf(ios::fixed);
            out.setf(ios::showpoint);
            out.precision(4);
            out.setf(ios::left);
            out.setf(ios::scientific);

            //Write data for Phi=0
            out << setw(12) << "0000" << setw(10) <<
                    sample.Voc << setw(10) << sample.NVoc <<
                    setw(10) << sample.current << setw(10) <<
                    sample.NormI << setw(10) <<  sample.Vmp <<
                    setw(10) << sample.Imp << setw(10) <<
```

```cpp
                sample.FF << setw(10) << sample.NFF <<
                setw(10) << sample.efficiency <<
                setw(10) << sample.Nefficiency << endl;

        //define counter var.
        double i = 0;

        //determine interval for Phi
        double interval  = (endFluence - begFluence) / dataPoints;

        //For each value of Phi, make calculations and write to file
        for(i = begFluence; i <= endFluence; i = i + interval)
        {
                //set value of Phi
                sample.setPhi(i);

                //Make Calculations
                sample.runCalcs();

                //Format Numbers
                out.setf(ios::fixed);
                out.setf(ios::showpoint);
                out.precision(4);
                out.setf(ios::left);
                out.setf(ios::scientific);

                //Write Data to file
                out << setw(12) << i << setw(10) <<
                        sample.Voc << setw(10) << sample.NVoc <<
                        setw(10) << sample.current <<
                        setw(10) << sample.NormI <<
                        setw(10) <<  sample.Vmp << setw(10) <<
                        sample.Imp << setw(10) << sample.FF <<
                        setw(10) << sample.NFF << setw(10) <<
                        sample.efficiency << setw(10) <<
                        sample.Nefficiency << endl;
        }
        //Close output file
        out.close();
}
```

fluence.h

```cpp
//Jacob Dunken
//CIGS Calcs
//Thesis Project

//fluence.h

#ifndef _FLUENCE_H //if it is isn't defined, define it..
#define _FLUENCE_H

class Fluence
{
private:

        void calcN();
        void calcVOC();
        void calcNVOC();
        void calcI();
        void calcDarkI();
        void calcVmp();
        void calcImp();
        void calcFF();
        void calcNFF();
        void calcEff();
        void calcNEff();
        void calcSeriesR();


        double mobHole, mobElec;
        double darkI;
        double ni;
        double resistivity;
        double q;
        double RSeries;
        double Pin;
        double Nc, Nv, Eg;
        double Voc0, current0, FF0, efficiency0;
        double N;


public:
        Fluence();
        void runCalcs();
        void setPhi(double uPhi);
        void setDefRate(double uDefRate);

        double Vmp, Imp;
        double FF, NFF;
        double Phi, DefRate, current, NormI;
        double NA, Voc, NVoc;
        double efficiency, Nefficiency;
};
#endif
```

fluence.cpp

```cpp
//Jacob Dunken
//CIGS Calcs
//Thesis Project

//fluence.cpp

#include <cmath> //for math functions
using namespace std;
#include "calculator.h"
#include "fluence.h"


Fluence::Fluence()
{
     //Initialize Variables
     NA = 0;
     Voc = 0;
     NVoc = 0;
     N = 0;
     mobHole = 25;
     mobElec = 100;
     darkI = 0;
     resistivity = 0;
     RSeries = 0;
     FF = 0;
     NFF = 0;
     efficiency = 0;
     Nefficiency = 0;
     Pin = 0.100;
     Vmp = 0.001;
     Imp = 0.0;
     ni = 0;

}
//set fluence
void Fluence::setPhi(double uPhi)
{
     Phi = uPhi;
}
//set defect introduction rate
void Fluence::setDefRate(double uDefRate)
{
     DefRate = uDefRate;
}


void Fluence::runCalcs()
{
     //Set Variables
     NA = 2.0e+16;
     q = 1.6E-19;
```

```cpp
        Nc = 2.2E+18;
        Nv = 1.8E+19;
        Eg = 1.15;
        ni = Nc * Nv *exp(-Eg/0.0259);

        //Calculate Defect Density
        calcN();
}


void Fluence::calcN()
{
        N = 0; //Initialize N

        //Calculate Defect Density
        N = 4.0E+15 + (DefRate * Phi);
        calcVOC();
}
void Fluence::calcVOC() //Calculate Voc.
{

        Voc = 0; //Inititalize Var.

        //Calc. Voc
        Voc = 0.640 - 1.8*0.0259*log(1 + ((DefRate * Phi) / 4E+15));

        //If Phi=0, just set Voc to initial cond. and calc. Norm. Voc.
        //Otherwise just go to calc. Norm. Voc.
        if (Phi == 0)
        {
                Voc0 = Voc;
                calcNVOC();
        }
        else
        {
                calcNVOC();
        }
}
void Fluence::calcNVOC() //Calc. Norm. Voc.
{
        NVoc = 0; //Initialize
        NVoc = Voc/Voc0; //Calc.
        calcI();
}
void Fluence::calcI() //Calculate Current (Isc)
{
        //Initialize Variables
        current = 0;
        NormI = 0;

        // Calc Current
        current = (0.031*0.5) * exp((-1.6E-16 * Phi) / (0.031));


        //if Phi = 0, set Isc to init. value and calc Norm = 1
```

```cpp
        if (Phi == 0)
        {
                current0 = current;
                NormI = current / current0;
                calcDarkI();
        }
        else //otherwise calc. Norm. Current
        {
                NormI = current / current0;
                calcDarkI();
        }
}
void Fluence::calcDarkI() //Calc. Dark Current
{
        darkI = 0; //Init. Var.

        //Calc. Dark Current
        darkI = current / (exp(Voc/0.0259)-1);

        calcVmp();
}
void Fluence::calcVmp() //Calc. Max. Power Voltage
{
        Vmp = 0; //Initialize Var.

        double max = 0.00001; //Value used for comparison to solve for
Vmp

        //Solve for Vmp, Calc. a value and set equal to max.
        //When within a certain margin of error will have Vmp.
        do
        {
                max = Voc - 0.0259 * log((Vmp / 0.0259) + 1);
                Vmp = Vmp + 0.00001;
        }while((max >= (Vmp-0.000001)));
        calcImp();
}

void Fluence::calcImp() //Calc. Max. Power Current
{
        Imp = 0; //Init. Var.

        //Calc. Current
        Imp = current- (darkI * (exp(Vmp / 0.0259) - 1));

        calcSeriesR();
}
void Fluence::calcSeriesR() //Calc. Rs
{
        //Find degraded value of NA
        double NA2 = NA*exp((-1650*Phi) / NA);

        //Calc. Resistivity
        resistivity = 1 / ((q * NA2 * mobHole)+(q * ni/NA2 * mobElec));
```

```cpp
        //calc. Resistance
        double R = resistivity * (2.0E-04 / 0.5);

        //Find Characteristic Resistance
        double Rch = Voc / current;

        //Find normalized Resistance
        RSeries = R / Rch;

        calcFF();
}
void Fluence::calcFF() //Calculate Fill Factor
{
        FF = 0; //Init. Var.

        //Calc. FF
        FF = (Vmp * Imp) / (Voc * current);

        //Take into account Rs
        FF = FF * (1 - RSeries);

        //If Phi=0, set FF to init. value, and calc. Norm. FF.
        //otherwise just calc. Norm. FF
        if (Phi == 0)
        {
                FF0 = FF;
                calcNFF();
        }
        else
        {
                calcNFF();
        }
}
void Fluence::calcNFF() //Calc. Norm. FF
{
        NFF = 0; //Init. Var.

        NFF = FF / FF0;

        calcEff();
}
void Fluence::calcEff() //Calc. Efficiency
{
        efficiency = 0; //Init. Var.

        //Calc. Eff.
        efficiency = (Voc * current * FF) / Pin;

        //If Phi=0, set Eff. to init. value, and calc. Norm. Eff.
        //otherwise just calc. Norm. Eff.
        if (Phi == 0)
        {
                efficiency0 = efficiency;
                calcNEff();
        }
```

```cpp
        else
        {
            calcNEff();
        }
}
void Fluence::calcNEff() //Calc. Norm. Eff.
{
        Nefficiency = 0; //Init. Var.

        //Calc. Norm. Eff.
        Nefficiency = efficiency / efficiency0;
}
```

APPENDIX C – CALCULATION OF THE DEFECT INTRODUCTION RATE

FOR 290 KEV PROTONS

TARGET DEPTH (Ang.)	Cu Vacancies	In Vacancies	Ga Vacancies	Se Vacancies	Sum of Vacancies	Vac.-cm/ Ion
2.40E+02	0.00E+00	0.00E+00	0.00E+00	0.00E+00		
4.80E+02	0.00E+00	0.00E+00	0.00E+00	0.00E+00		
7.20E+02	0.00E+00	0.00E+00	0.00E+00	0.00E+00		
9.60E+02	0.00E+00	0.00E+00	0.00E+00	0.00E+00		
1.20E+03	0.00E+00	0.00E+00	0.00E+00	0.00E+00		
1.44E+03	0.00E+00	0.00E+00	0.00E+00	0.00E+00		
1.68E+03	0.00E+00	0.00E+00	0.00E+00	0.00E+00		
1.92E+03	0.00E+00	0.00E+00	0.00E+00	0.00E+00		
2.16E+03	0.00E+00	0.00E+00	0.00E+00	0.00E+00		
2.40E+03	0.00E+00	0.00E+00	0.00E+00	0.00E+00		
2.64E+03	0.00E+00	0.00E+00	0.00E+00	0.00E+00		
2.88E+03	0.00E+00	0.00E+00	0.00E+00	0.00E+00		
3.12E+03	0.00E+00	0.00E+00	0.00E+00	0.00E+00		
3.36E+03	0.00E+00	0.00E+00	0.00E+00	0.00E+00		
3.60E+03	0.00E+00	0.00E+00	0.00E+00	0.00E+00		
3.84E+03	0.00E+00	0.00E+00	0.00E+00	0.00E+00		
4.08E+03	1.96E-05	1.48E-05	3.88E-06	3.60E-05	7.43E-05	7.43E+03
4.32E+03	5.52E-05	5.01E-05	1.22E-05	1.10E-04	2.28E-04	2.28E+04
4.56E+03	7.99E-05	7.64E-05	1.77E-05	1.66E-04	3.40E-04	3.40E+04
4.80E+03	8.42E-05	7.78E-05	1.89E-05	1.71E-04	3.52E-04	3.52E+04
5.04E+03	8.83E-05	8.15E-05	2.00E-05	1.91E-04	3.81E-04	3.81E+04
5.28E+03	1.04E-04	9.26E-05	2.40E-05	2.11E-04	4.31E-04	4.31E+04
5.52E+03	8.95E-05	8.95E-05	2.08E-05	1.97E-04	3.97E-04	3.97E+04
5.76E+03	1.10E-04	1.01E-04	2.24E-05	2.33E-04	4.67E-04	4.67E+04
6.00E+03	1.13E-04	9.99E-05	2.44E-05	2.35E-04	4.72E-04	4.72E+04
6.24E+03	1.07E-04	1.01E-04	2.53E-05	2.28E-04	4.61E-04	4.61E+04
6.48E+03	1.10E-04	1.02E-04	2.45E-05	2.25E-04	4.62E-04	4.62E+04
6.72E+03	1.01E-04	9.32E-05	2.17E-05	2.07E-04	4.22E-04	4.22E+04
6.96E+03	9.82E-05	9.43E-05	2.21E-05	2.12E-04	4.27E-04	4.27E+04
7.20E+03	1.10E-04	1.05E-04	2.51E-05	2.29E-04	4.69E-04	4.69E+04
7.44E+03	1.11E-04	1.05E-04	2.51E-05	2.44E-04	4.85E-04	4.85E+04
7.68E+03	1.10E-04	1.04E-04	2.44E-05	2.31E-04	4.69E-04	4.69E+04
7.92E+03	1.06E-04	9.58E-05	2.29E-05	2.27E-04	4.51E-04	4.51E+04
8.16E+03	1.08E-04	1.02E-04	2.34E-05	2.32E-04	4.65E-04	4.65E+04
8.40E+03	1.05E-04	9.60E-05	2.18E-05	2.18E-04	4.40E-04	4.40E+04
8.64E+03	1.15E-04	1.05E-04	2.57E-05	2.39E-04	4.85E-04	4.85E+04
8.88E+03	1.11E-04	1.08E-04	2.53E-05	2.37E-04	4.82E-04	4.82E+04
9.12E+03	1.07E-04	1.03E-04	2.59E-05	2.32E-04	4.67E-04	4.67E+04
9.36E+03	1.16E-04	1.10E-04	2.50E-05	2.44E-04	4.96E-04	4.96E+04
9.60E+03	1.07E-04	9.89E-05	2.37E-05	2.24E-04	4.53E-04	4.53E+04
9.84E+03	1.11E-04	1.00E-04	2.56E-05	2.33E-04	4.70E-04	4.70E+04
1.01E+04	1.21E-04	1.09E-04	2.53E-05	2.50E-04	5.06E-04	5.06E+04
1.03E+04	1.10E-04	1.06E-04	2.45E-05	2.36E-04	4.77E-04	4.77E+04
1.06E+04	1.18E-04	1.14E-04	2.80E-05	2.48E-04	5.08E-04	5.08E+04
1.08E+04	1.19E-04	1.14E-04	2.61E-05	2.54E-04	5.12E-04	5.12E+04
1.10E+04	1.12E-04	1.05E-04	2.34E-05	2.34E-04	4.75E-04	4.75E+04
1.13E+04	1.15E-04	1.10E-04	2.61E-05	2.42E-04	4.93E-04	4.93E+04
1.15E+04	1.23E-04	1.16E-04	2.80E-05	2.64E-04	5.31E-04	5.31E+04
1.18E+04	1.28E-04	1.17E-04	2.60E-05	2.60E-04	5.30E-04	5.30E+04
1.20E+04	1.21E-04	1.11E-04	2.65E-05	2.51E-04	5.08E-04	5.08E+04

1.22E+04	1.22E-04	1.15E-04	2.73E-05	2.53E-04	5.16E-04	5.16E+04
1.25E+04	1.19E-04	1.12E-04	2.64E-05	2.40E-04	4.97E-04	4.97E+04
1.27E+04	1.23E-04	1.13E-04	2.66E-05	2.57E-04	5.20E-04	5.20E+04
1.30E+04	1.21E-04	1.13E-04	2.61E-05	2.51E-04	5.10E-04	5.10E+04
1.32E+04	1.17E-04	1.09E-04	2.48E-05	2.45E-04	4.96E-04	4.96E+04
1.34E+04	1.16E-04	1.04E-04	2.63E-05	2.33E-04	4.79E-04	4.79E+04
1.37E+04	1.20E-04	1.07E-04	2.56E-05	2.51E-04	5.03E-04	5.03E+04
1.39E+04	1.20E-04	1.09E-04	2.78E-05	2.53E-04	5.10E-04	5.10E+04
1.42E+04	1.04E-04	9.75E-05	2.40E-05	2.28E-04	4.53E-04	4.53E+04
1.44E+04	1.15E-04	1.05E-04	2.56E-05	2.41E-04	4.87E-04	4.87E+04
1.46E+04	1.08E-04	9.87E-05	2.49E-05	2.31E-04	4.62E-04	4.62E+04
1.49E+04	1.16E-04	1.03E-04	2.80E-05	2.35E-04	4.83E-04	4.83E+04
1.51E+04	1.03E-04	9.14E-05	2.19E-05	2.11E-04	4.27E-04	4.27E+04
1.54E+04	9.94E-05	9.23E-05	2.05E-05	2.11E-04	4.23E-04	4.23E+04
1.56E+04	1.01E-04	9.21E-05	2.23E-05	2.14E-04	4.29E-04	4.29E+04
1.58E+04	9.78E-05	8.90E-05	2.08E-05	2.00E-04	4.08E-04	4.08E+04
1.61E+04	9.36E-05	8.25E-05	2.00E-05	1.92E-04	3.88E-04	3.88E+04
1.63E+04	9.01E-05	8.25E-05	1.89E-05	1.84E-04	3.76E-04	3.76E+04
1.66E+04	9.00E-05	7.76E-05	2.03E-05	1.86E-04	3.74E-04	3.74E+04
1.68E+04	8.51E-05	8.03E-05	1.58E-05	1.76E-04	3.57E-04	3.57E+04
1.70E+04	8.00E-05	7.31E-05	1.82E-05	1.70E-04	3.41E-04	3.41E+04
1.73E+04	8.36E-05	7.30E-05	1.83E-05	1.63E-04	3.38E-04	3.38E+04
1.75E+04	7.50E-05	6.76E-05	1.53E-05	1.59E-04	3.17E-04	3.17E+04
1.78E+04	6.73E-05	6.20E-05	1.52E-05	1.44E-04	2.89E-04	2.89E+04
1.80E+04	6.83E-05	6.27E-05	1.50E-05	1.38E-04	2.84E-04	2.84E+04
1.82E+04	6.06E-05	5.07E-05	1.34E-05	1.24E-04	2.49E-04	2.49E+04
1.85E+04	6.24E-05	5.32E-05	1.40E-05	1.28E-04	2.58E-04	2.58E+04
1.87E+04	5.88E-05	5.09E-05	1.30E-05	1.20E-04	2.43E-04	2.43E+04
1.90E+04	5.25E-05	4.63E-05	1.06E-05	1.09E-04	2.19E-04	2.19E+04
1.92E+04	5.03E-05	4.76E-05	1.08E-05	1.03E-04	2.11E-04	2.11E+04
1.94E+04	4.38E-05	3.78E-05	9.42E-06	9.31E-05	1.84E-04	1.84E+04
1.97E+04	4.19E-05	3.75E-05	8.50E-06	8.75E-05	1.75E-04	1.75E+04
1.99E+04	3.43E-05	3.53E-05	7.54E-06	7.63E-05	1.53E-04	1.53E+04
2.02E+04	3.80E-05	3.43E-05	7.83E-06	7.68E-05	1.57E-04	1.57E+04
2.04E+04	3.27E-05	2.86E-05	8.00E-06	6.67E-05	1.36E-04	1.36E+04
2.06E+04	3.18E-05	2.64E-05	6.63E-06	6.36E-05	1.28E-04	1.28E+04
2.09E+04	2.83E-05	2.36E-05	6.38E-06	5.64E-05	1.15E-04	1.15E+04
2.11E+04	2.67E-05	2.09E-05	5.88E-06	5.25E-05	1.06E-04	1.06E+04
2.14E+04	2.20E-05	1.95E-05	5.08E-06	4.81E-05	9.47E-05	9.47E+03
2.16E+04	2.14E-05	2.11E-05	5.25E-06	4.58E-05	9.35E-05	9.35E+03
2.18E+04	2.00E-05	1.56E-05	4.38E-06	3.93E-05	7.93E-05	7.93E+03
2.21E+04	1.87E-05	1.55E-05	3.88E-06	3.59E-05	7.40E-05	7.40E+03
2.23E+04	1.49E-05	1.25E-05	3.88E-06	3.35E-05	6.48E-05	6.48E+03
2.26E+04	1.72E-05	1.27E-05	4.04E-06	3.07E-05	6.46E-05	6.46E+03
2.28E+04	1.36E-05	1.09E-05	2.83E-06	2.79E-05	5.52E-05	5.52E+03
2.30E+04	1.15E-05	1.04E-05	2.33E-06	2.30E-05	4.72E-05	4.72E+03
2.33E+04	7.46E-06	7.79E-06	2.04E-06	1.66E-05	3.39E-05	3.39E+03
2.35E+04	7.83E-06	6.08E-06	1.92E-06	1.39E-05	2.97E-05	2.97E+03
2.38E+04	7.71E-06	5.13E-06	1.46E-06	1.23E-05	2.65E-05	2.65E+03
2.40E+04	5.46E-06	5.50E-06	1.33E-06	1.27E-05	2.50E-05	2.50E+03
			Defect Introduction Rate:			3.43E+04

APPENDIX D – TRIM.DAT EXCERPT (290 KEV)

Jacob Dunken								
Date: 5/28/07								
The atomic number of the ion is>>1								
Event #	Atom #	Energy(eV	X(Ang)	Y(Ang)	Z(Ang)	Cos(X)	Cos(Y)	Cos(Z)
0	1	290000	0	1083	-4944	0.6561	0.766	-0.9962
1	1	290000	0	1397	-3649	0.0872	-0.9816	-0.9998
2	1	290000	0	-1056	-2354	-0.6293	-0.454	0.9994
3	1	290000	0	-741	-1058	-0.9703	0.4226	0.9962
4	1	290000	0	-427	3005	0.866	0.9945	0.9903
5	1	290000	0	3407	-4838	0.3907	-0.0349	-0.9945
6	1	290000	0	-2923	3718	-0.6691	0.6428	0.4384
7	1	290000	0	-576	2055	-0.9816	0.0523	-0.9781
8	1	290000	0	2534	4205	0.0349	0.9962	0.3256
9	1	290000	0	-1828	4167	0.309	0.9925	0.4226
10	1	290000	0	-3627	194	-0.1392	0.1045	-0.309
11	1	290000	0	1053	3596	0.309	-0.6561	-0.8387
12	1	290000	0	1764	4067	-0.682	-0.866	0.7431
13	1	290000	0	4593	-2867	-0.9962	0.5299	-0.9994
14	1	290000	0	-3593	1743	-0.1564	0.0872	0.9994
15	1	290000	0	3850	-1394	-0.829	0.9945	-0.866
16	1	290000	0	3431	-168	-0.891	0.515	-0.6691
17	1	290000	0	-2597	4859	-0.9455	-0.6157	-0.6947
18	1	290000	0	3924	-904	-0.866	0.9455	-0.9925
19	1	290000	0	-1314	4253	-0.3746	-0.0523	0.6293
20	1	290000	0	-2683	2842	-0.7431	0.7431	0.8387
21	1	290000	0	1195	1204	-0.9781	-0.9781	0.8572
22	1	290000	0	-4348	2381	0.6157	0.1564	-0.8387
23	1	290000	0	4136	-1101	0.8387	0.6428	-0.7071
24	1	290000	0	-4529	-1522	0	0.7771	0.6691
25	1	290000	0	3358	-716	0.1219	0.6157	0.9848
26	1	290000	0	-878	793	0.7071	0.9816	0.4384
27	1	290000	0	-3453	-3655	-0.5592	-0.2419	-0.6947
28	1	290000	0	-3984	-4154	0.848	-0.5446	0.9744
29	1	290000	0	-457	256	-0.7071	-0.1219	0.6428
30	1	290000	0	-4478	-996	0.9703	0.9848	-0.309
31	1	290000	0	-3129	4100	0.0872	-0.5736	0.9135
32	1	290000	0	2525	1678	0.766	0.6947	0.2419
33	1	290000	0	-3088	2858	-0.2079	-0.682	-0.2079
34	1	290000	0	2849	-1087	0.342	0.7314	-0.7193
35	1	290000	0	-3533	-4515	-0.0175	-0.8746	-0.8192
36	1	290000	0	-1907	-977	0.4695	0.8387	-0.9455

APPENDIX E – CIGS CALCULATOR OUTPUT FOR 290 KEV PROTONS

CIGS Calculator										
Jacob Dunnen										
PHI	Voc	NVoc	current	NormI	Vmp	Imp	FF	NFF	Efficiency	Nefficiency
0	0.64	1	0.0155	1	0.5593	0.01481	0.8351	1	0.08284	1
1.00E+11	0.6111	0.9549	0.01549	0.9995	0.5316	0.01477	0.8294	0.9932	0.07853	0.9479
1.10E+12	0.5307	0.8292	0.01541	0.9943	0.4551	0.01458	0.8111	0.9713	0.06635	0.8009
2.10E+12	0.5028	0.7856	0.01533	0.9892	0.4286	0.01446	0.8037	0.9624	0.06195	0.7479
3.10E+12	0.4854	0.7584	0.01525	0.9841	0.4122	0.01435	0.7987	0.9565	0.05914	0.7139
4.10E+12	0.4728	0.7387	0.01518	0.9791	0.4003	0.01425	0.7949	0.952	0.05704	0.6885
5.10E+12	0.4629	0.7232	0.0151	0.974	0.3909	0.01416	0.7919	0.9483	0.05534	0.668
6.09E+12	0.4547	0.7104	0.01502	0.969	0.3832	0.01407	0.7892	0.9451	0.0539	0.6507
7.09E+12	0.4477	0.6996	0.01494	0.9641	0.3767	0.01398	0.7869	0.9424	0.05265	0.6356
8.09E+12	0.4417	0.6901	0.01487	0.9591	0.371	0.0139	0.7849	0.9399	0.05153	0.6221
9.09E+12	0.4363	0.6818	0.01479	0.9542	0.366	0.01381	0.783	0.9377	0.05053	0.61
1.01E+13	0.4315	0.6743	0.01471	0.9493	0.3615	0.01373	0.7813	0.9357	0.04961	0.5989
1.11E+13	0.4272	0.6674	0.01464	0.9444	0.3574	0.01365	0.7798	0.9338	0.04876	0.5886
1.21E+13	0.4232	0.6612	0.01456	0.9395	0.3537	0.01357	0.7783	0.932	0.04796	0.579
1.31E+13	0.4195	0.6555	0.01449	0.9347	0.3502	0.01349	0.7769	0.9304	0.04722	0.57
1.41E+13	0.4161	0.6502	0.01441	0.9299	0.347	0.01341	0.7756	0.9289	0.04652	0.5616
1.51E+13	0.4129	0.6452	0.01434	0.9251	0.3441	0.01334	0.7744	0.9274	0.04586	0.5536
1.61E+13	0.41	0.6406	0.01427	0.9203	0.3413	0.01326	0.7733	0.926	0.04522	0.5459
1.71E+13	0.4072	0.6362	0.01419	0.9156	0.3387	0.01318	0.7722	0.9247	0.04462	0.5387
1.81E+13	0.4046	0.6321	0.01412	0.9109	0.3363	0.01311	0.7711	0.9234	0.04404	0.5317
1.91E+13	0.4021	0.6282	0.01405	0.9062	0.3339	0.01304	0.7701	0.9222	0.04349	0.525
2.01E+13	0.3997	0.6245	0.01397	0.9016	0.3317	0.01296	0.7691	0.921	0.04296	0.5186
2.11E+13	0.3975	0.621	0.0139	0.8969	0.3296	0.01289	0.7681	0.9199	0.04244	0.5124
2.21E+13	0.3953	0.6177	0.01383	0.8923	0.3276	0.01282	0.7672	0.9187	0.04195	0.5064
2.31E+13	0.3933	0.6145	0.01376	0.8877	0.3257	0.01275	0.7663	0.9177	0.04146	0.5006
2.41E+13	0.3913	0.6114	0.01369	0.8831	0.3239	0.01267	0.7654	0.9166	0.041	0.4949
2.51E+13	0.3894	0.6084	0.01362	0.8786	0.3221	0.0126	0.7646	0.9156	0.04055	0.4895
2.61E+13	0.3876	0.6056	0.01355	0.8741	0.3204	0.01253	0.7637	0.9146	0.04011	0.4841
2.71E+13	0.3858	0.6029	0.01348	0.8696	0.3188	0.01247	0.7629	0.9136	0.03968	0.479
2.81E+13	0.3842	0.6003	0.01341	0.8651	0.3172	0.0124	0.7621	0.9127	0.03926	0.4739
2.91E+13	0.3825	0.5977	0.01334	0.8607	0.3157	0.01233	0.7613	0.9117	0.03885	0.469

3.01E+13	0.381	0.5953	0.01327	0.8562	0.3143	0.01226	0.7605	0.9108	0.03845	0.4642
3.11E+13	0.3794	0.5929	0.0132	0.8518	0.3129	0.01219	0.7598	0.9098	0.03806	0.4595
3.21E+13	0.378	0.5906	0.01314	0.8475	0.3115	0.01213	0.759	0.9089	0.03768	0.4549
3.31E+13	0.3766	0.5884	0.01307	0.8431	0.3102	0.01206	0.7582	0.908	0.03731	0.4504
3.41E+13	0.3752	0.5862	0.013	0.8388	0.3089	0.01199	0.7574	0.9071	0.03694	0.446
3.51E+13	0.3738	0.5841	0.01293	0.8345	0.3077	0.01193	0.7567	0.9061	0.03659	0.4417
3.61E+13	0.3725	0.5821	0.01287	0.8302	0.3064	0.01186	0.7559	0.9052	0.03623	0.4374
3.71E+13	0.3713	0.5801	0.0128	0.8259	0.3053	0.0118	0.7551	0.9043	0.03589	0.4332
3.81E+13	0.37	0.5782	0.01274	0.8216	0.3041	0.01174	0.7544	0.9034	0.03555	0.4291
3.91E+13	0.3688	0.5763	0.01267	0.8174	0.303	0.01167	0.7536	0.9024	0.03521	0.4251
4.01E+13	0.3676	0.5744	0.0126	0.8132	0.3019	0.01161	0.7528	0.9015	0.03488	0.4211
4.11E+13	0.3665	0.5726	0.01254	0.809	0.3009	0.01155	0.752	0.9005	0.03456	0.4172
4.21E+13	0.3654	0.5709	0.01248	0.8049	0.2998	0.01148	0.7511	0.8995	0.03424	0.4133
4.31E+13	0.3643	0.5692	0.01241	0.8007	0.2988	0.01142	0.7503	0.8985	0.03392	0.4095
4.41E+13	0.3632	0.5675	0.01235	0.7966	0.2978	0.01136	0.7494	0.8975	0.03361	0.4058
4.51E+13	0.3622	0.5659	0.01228	0.7925	0.2969	0.0113	0.7486	0.8964	0.0333	0.402
4.61E+13	0.3612	0.5643	0.01222	0.7884	0.2959	0.01124	0.7477	0.8954	0.033	0.3984
4.71E+13	0.3602	0.5627	0.01216	0.7844	0.295	0.01118	0.7467	0.8942	0.0327	0.3947
4.81E+13	0.3592	0.5612	0.0121	0.7804	0.2941	0.01112	0.7458	0.8931	0.0324	0.3911
4.91E+13	0.3582	0.5597	0.01203	0.7763	0.2932	0.01106	0.7448	0.8919	0.0321	0.3876
5.01E+13	0.3573	0.5583	0.01197	0.7723	0.2923	0.011	0.7437	0.8907	0.03181	0.384
5.11E+13	0.3564	0.5568	0.01191	0.7684	0.2915	0.01094	0.7427	0.8894	0.03152	0.3805
5.21E+13	0.3555	0.5554	0.01185	0.7644	0.2906	0.01088	0.7415	0.888	0.03123	0.377
5.31E+13	0.3546	0.554	0.01179	0.7605	0.2898	0.01082	0.7404	0.8866	0.03095	0.3736
5.41E+13	0.3537	0.5527	0.01173	0.7566	0.289	0.01076	0.7391	0.8851	0.03066	0.3701
5.51E+13	0.3529	0.5513	0.01167	0.7527	0.2882	0.0107	0.7379	0.8836	0.03038	0.3667
5.60E+13	0.352	0.55	0.01161	0.7488	0.2875	0.01065	0.7365	0.882	0.03009	0.3633
5.70E+13	0.3512	0.5488	0.01155	0.745	0.2867	0.01059	0.7351	0.8803	0.02981	0.3599
5.80E+13	0.3504	0.5475	0.01149	0.7411	0.286	0.01053	0.7336	0.8785	0.02953	0.3565
5.90E+13	0.3496	0.5463	0.01143	0.7373	0.2852	0.01048	0.732	0.8766	0.02925	0.353
6.00E+13	0.3488	0.545	0.01137	0.7335	0.2845	0.01042	0.7303	0.8745	0.02896	0.3496
6.10E+13	0.3481	0.5438	0.01131	0.7298	0.2838	0.01037	0.7285	0.8724	0.02868	0.3462
6.20E+13	0.3473	0.5427	0.01125	0.726	0.2831	0.01031	0.7266	0.8701	0.0284	0.3428
6.30E+13	0.3466	0.5415	0.0112	0.7223	0.2824	0.01025	0.7246	0.8677	0.02811	0.3394
6.40E+13	0.3458	0.5403	0.01114	0.7186	0.2817	0.0102	0.7224	0.8651	0.02782	0.3359
6.50E+13	0.3451	0.5392	0.01108	0.7149	0.2811	0.01015	0.7201	0.8624	0.02754	0.3324
6.60E+13	0.3444	0.5381	0.01102	0.7112	0.2804	0.01009	0.7177	0.8594	0.02725	0.3289
6.70E+13	0.3437	0.537	0.01097	0.7075	0.2798	0.01004	0.715	0.8563	0.02695	0.3254
6.80E+13	0.343	0.5359	0.01091	0.7039	0.2791	0.009984	0.7123	0.8529	0.02665	0.3218
6.90E+13	0.3423	0.5349	0.01085	0.7003	0.2785	0.009931	0.7093	0.8494	0.02635	0.3181

7.00E+13	0.3417	0.5338	0.0108	0.6967	0.2779	0.009877	0.706	0.8455	0.02605	0.3145
7.10E+13	0.341	0.5328	0.01074	0.6931	0.2773	0.009825	0.7026	0.8414	0.02574	0.3107
7.20E+13	0.3403	0.5318	0.01069	0.6895	0.2767	0.009773	0.6989	0.837	0.02542	0.3069
7.30E+13	0.3397	0.5308	0.01063	0.686	0.2761	0.009721	0.6949	0.8322	0.0251	0.303
7.40E+13	0.3391	0.5298	0.01058	0.6824	0.2755	0.009669	0.6907	0.8271	0.02477	0.2991
7.50E+13	0.3385	0.5288	0.01052	0.6789	0.2749	0.009617	0.6861	0.8216	0.02444	0.295
7.60E+13	0.3378	0.5279	0.01047	0.6754	0.2744	0.009566	0.6812	0.8158	0.02409	0.2909
7.70E+13	0.3372	0.5269	0.01042	0.672	0.2738	0.009515	0.6759	0.8094	0.02374	0.2866
7.80E+13	0.3366	0.526	0.01036	0.6685	0.2733	0.009465	0.6702	0.8026	0.02338	0.2822
7.90E+13	0.336	0.5251	0.01031	0.6651	0.2727	0.009414	0.6641	0.7953	0.023	0.2777
8.00E+13	0.3355	0.5241	0.01026	0.6617	0.2722	0.009364	0.6575	0.7874	0.02262	0.2731
8.10E+13	0.3349	0.5232	0.0102	0.6583	0.2717	0.009315	0.6504	0.7788	0.02222	0.2682
8.20E+13	0.3343	0.5223	0.01015	0.6549	0.2711	0.009265	0.6427	0.7696	0.02181	0.2633
8.30E+13	0.3337	0.5215	0.0101	0.6515	0.2706	0.009216	0.6344	0.7598	0.02138	0.2581
8.40E+13	0.3332	0.5206	0.01005	0.6482	0.2701	0.009167	0.6255	0.7491	0.02094	0.2528
8.50E+13	0.3326	0.5197	0.009995	0.6448	0.2696	0.009118	0.6159	0.7376	0.02048	0.2472
8.60E+13	0.3321	0.5189	0.009943	0.6415	0.2691	0.00907	0.6055	0.7251	0.02	0.2414
8.70E+13	0.3316	0.518	0.009892	0.6382	0.2686	0.009022	0.5943	0.7117	0.01949	0.2353
8.80E+13	0.331	0.5172	0.009841	0.6349	0.2681	0.008974	0.5823	0.6973	0.01897	0.229
8.90E+13	0.3305	0.5164	0.009791	0.6317	0.2676	0.008927	0.5692	0.6817	0.01842	0.2224
9.00E+13	0.33	0.5156	0.00974	0.6284	0.2672	0.008879	0.5552	0.6648	0.01784	0.2154
9.10E+13	0.3295	0.5148	0.00969	0.6252	0.2667	0.008832	0.54	0.6466	0.01724	0.2081
9.20E+13	0.329	0.514	0.00964	0.622	0.2662	0.008785	0.5236	0.627	0.0166	0.2004
9.30E+13	0.3284	0.5132	0.009591	0.6188	0.2657	0.008739	0.5058	0.6058	0.01593	0.1924
9.40E+13	0.328	0.5124	0.009541	0.6156	0.2653	0.008693	0.4867	0.5828	0.01523	0.1838
9.50E+13	0.3275	0.5117	0.009492	0.6124	0.2648	0.008646	0.466	0.5581	0.01449	0.1749
9.60E+13	0.327	0.5109	0.009444	0.6093	0.2644	0.008601	0.4437	0.5313	0.0137	0.1654
9.70E+13	0.3265	0.5101	0.009395	0.6061	0.264	0.008555	0.4196	0.5024	0.01287	0.1554
9.80E+13	0.326	0.5094	0.009347	0.603	0.2635	0.00851	0.3935	0.4712	0.01199	0.1447
9.90E+13	0.3255	0.5087	0.009299	0.5999	0.2631	0.008465	0.3653	0.4375	0.01106	0.1335
1.00E+14	0.3251	0.5079	0.009251	0.5968	0.2627	0.00842	0.3349	0.401	0.01007	0.1216

REFERENCES

[1]   J. Nelson, *The Physics of Solar Cells*. London, UK: Imperial College Press, 2003.

[2]   M.A. Green, *Solar Cells: Operating Principles, Technology and System Applications.* Kensington, NSW, Australia: The University of New South Wales, 1998.

[3]   Standard Solar Constant and Zero Air Mass Solar Spectral Irradiance Tables, ASTM Standard E490-00a, 2000 (2006).

[4]   BP Solar, "BP 175B 175 Watt Photovoltaic Module," April 2006, http://www.bp.com/liveassets/bp_internet/solar/bp_solar_north_america/STAGIN G/local_assets/downloads_pdfs/BP_175B_datasheet_10_06.pdf.

[5]   BP Solar, "BP 4175 175 Watt Photovoltaic Module," September 2004, http://www.bp.com/liveassets/bp_internet/solar/bp_solar_north_america/STAGIN G/local_assets/downloads_pdfs/pq/product_data_sheet_4175B_en.pdf.

[6]   Sharp Electronics Corporation, "ND-208U1F Multi-Purpose Module*,*" 2006, http://solar.sharpusa.com/files/sol_dow_208U1F_ss.pdf.

[7]   Solar Home.org, "Global Solar," September 2007, http://www.globalsolar.com/dmdocuments/SL%2025%20Spec%20Sheet.pdf.

[8]   Global Solar, "SUNLINQ Portable Solar Panel – 25 Watt," August 2006, http://www.globalsolar.com/dmdocuments/SL%2025%20Spec%20Sheet.pdf.

[9]   D.C. Senft, "Opportunities in Photovoltaics for Space Power Generation," in *Conference Record of the Thirty-first IEEE Photovoltaic Specialist* Conference, Lake Buena Vista, FL, 2005, pp. 536-541.

[10]   A. Suzuki, M. Kaneiwa, T. Saga, and S. Matsuda. (1999, October). Progress and Future View of Silicon Space Solar Cells in Japan. *IEEE Transactions on Electron Devices* [Online]. *46(10)*, 2126-2132. Available: http://ieeexplore.ieee.org

[11]   R.R. King, C.M. Fetzer, D.C. Law, K.M. Edmondson, Hojun Yoon, G.S. Kinsey, D.D. Krut, J.H. Ermer, P. Hebert, B.T. Cavicchi, and N.H. Karam, "Advanced III-V Multijunction Cells for Space," in *Conference Record of the 2006 IEEE 4th World Conference on Photovoltaic Energy Conversion,* Waikoloa, HI, 2006, pp. 1757-1762.

[12]   J.M. Merrill, P. Hausgen, D. Senft, and J. Granata, "Air Force Perspective on Present and Future Space Power Generation," in *Conference Record of the 2006*

IEEE 4th World Conference on Photovoltaic Energy Conversion, Waikoloa, HI, 2006, pp. 1750-1756.

[13]   S.Kawakita, M. Imaizumi, T. Sumita, K. Kushiya, T. Ohshima, M. Yamaguchi, S. Matsuda, S. Yoda, and T. Kamiya, "Super Radiation Tolerance of CIGS Solar Cells Demonstrated in Space By MDS-1 Satellite," *in Proceedings of Third World Conference on Photovoltaic Energy Conversion*, Osaka, Japan, 2003, pp. 693-696.

[14]   International Solar Electric Technology, Inc., "Low Cost Photovoltaics – R&D for the Solar Energy Industry," October 2007, http://www.isetinc.com/research.html.

[15]   U. Rau, H.W. Schock, "Electronic Properties of Cu(In,Ga)Se$_2$ Heterojunction Solar Cells-Recent Achievements, Current Understanding, and Future Challenges," *Appl. Phys. A,* vol. 69, pp. 131-147, Jun., 1999.

[16]   M.A. Contreras, T. Nakada, M. Hongo, A.O. Pudov, and J.R. Sites, "ZnO/ZnS(O,OH)/Cu(In,Ga)Se$_2$/Mo Solar Cell with 18.6% Efficiency," in *Proceedings of Third World Conference on Photovoltaic Energy Conversion*, Osaka, Japan, 2003, pp. 570-573.

[17]   J.E. Granata, T.D. Sahlstrom, P.E. Hausgen, S.R. Messenger, J.R. Lorentzen, and R.J. Walters, "Thin-Film Photovoltaic Proton Radiation Testing for a MEO Orbit," in *Conference Record of the Thirty-first IEEE Photovoltaic Specialist Conference,* Lake Buena Vista, FL, 2005, pp. 607-610.

[18]   Wikipedia, "Low Earth Orbit," June 2007, http://en.wikipedia.org/wiki/Low_Earth_orbit

[19]   Wikipedia, "Medium Earth Orbit," June 2007, http://en.wikipedia.org/wiki/Medium_Earth_Orbit

[20]   Wikipedia, "Geosynchronous Orbit," June 2007, http://en.wikipedia.org/wiki/Geosynchronous_orbit

[21]   M.P. Petkov. (2003, January). New Millennium Program (NMP): Space Environments on Electronic Components Guidelines. NASA, Jet Propulsion Laboratory, California Institute of Technology. Pasadena, CA. [Online]. Available: http://nmp.jpl.nasa.gov/JOIN/NMP_Space_Env_Effects.pdf

[22]   J.E. Granata, private communication, Feb. 2006.

[23]   M. Gloeckler, "Numerical Modeling of CIGS Solar Cells: Definition of the Baseline and Explanation of Superposition Failure," M.S. thesis, Phys., CSU, Fort Collins, Co., 2003.

[24]   A. Baumann, Y. Bhargava, Z. X. Liu, G. Menet, J. Wilcox, University of California, Berkley, "Photovoltatic Technology Review," December 2004, http://socrates.berkeley.edu/~kammen/C226/Berkeley-C226-PVTechComp-Pres.pdf.

[25]   M. Gloeckler, A.L. Fahrenbruch, J.R. Sites, "Numerical Modeling of CIGS and CdTe Solar Cells: Setting the Baseline," in *Proceedings of Third World Conference on Photovoltaic Energy Conversion*, Osaka, Japan, 2003, pp. 491-494.

[26]   A. Rockett, "Performance-Limitations in Cu(In,Ga)Se$_2$ – Based Heterojunction Solar Cells," in *Conference Record of the Twenty-Ninth IEEE Photovoltaic Specialists Conference*, New Orleans, LA, 2002, pp. 587-591.

[27]   B.M. Kayes, F. Hasoon, P. Dippo, A. Balcioglu, F. Abulfotuh, "Influence of Na on the Electro-Optical Properties of Cu(In,Ga)Se$_2$," in *Conference Record of the Twenty-Sixth IEEE Photovoltaic Specialists Conference*, Anaheim, CA, 1997, pp. 479-482.

[28]   D. Rudmann, A. F. da Cunha, M. Kaelin, F. Kurdesau, H. Zogg, A. N. Tiwari, and G. Bilger, " Efficiency Enhancement of Cu(In,Ga)Se$_2$ Solar Cells Due to Post-Deposition Na Incorporation," *Appl. Phys. Lett.,* vol. 84, pp. 1129-1131, Feb., 2004.

[29]   Y. Hashimoto, T. Satoh, S. Shimakawa, and T. Negami, "High Efficiency Cigs Solar Cell On Flexible Stainless Steel," in *Proceedings of Third World Conference on Photovoltaic Energy Conversion*, Osaka, Japan, 2003, pp. 574-577.

[30]   Clark, C. Summers, J. Armstrong, "Innovative Flexible Lightweight Thin-Film Power Generation and Storage for Space Applications," in *35th Intersociety Energy Conversion Engineering Conference and Exhibit*, Las Vegas, NV, 2000, pp. 692-698.

[31]   C. Platzer-Bjorkman, J. Kessler, L. Stolt, "Atomic Layer Deposition of Zn(O,S) Buffer Layers for High Efficiency Cu(In,Ga)Se$_2$ Solar Cells," in *Proceedings of Third World Conference on Photovoltaic Energy Conversion*, Osaka, Japan, 2003, pp. 461-464.

[32]   N. Naghavi, S. Spiering, M. Powalla, D. Lincot, "Record Efficiencies for Dry Processed Cadmium Free CIGS Solar Sells with Indium Sulfide Buffer Layers

Prepared By Atomic Layer Deposition (ALD)," in *Proceedings of Third World Conference on Photovoltaic Energy Conversion*, Osaka, Japan, 2003, pp. 340-343.

[33] Wikipedia, "Cadmium," August 2007, http://en.wikipedia.org/wiki/Cadmium.

[34] D. Hariskos, S. Spiering, and M. Powalla. Buffer Layers in Cu(In,Ga)Se$_2$ Solar Cells and Modules. *Thin Solid Films* [Online]. *480*, pp 99-109. Available: http://www.sciencedirect.com.

[35] T. Nakada and M. Mizutani, "Improved Efficiency of Cu(In,Ga)Se$_2$ Thin Film Solar Cells with Chemically Deposited ZnS Buffer Layers By Air-Annealing-Formation of Homojunction By Solid Phase Diffusion," in *Conference Record of theTwenty-Eighth IEEE Photovoltaic Specialists Conference*, Anchorage, AK, 2000, pp. 529-534.

[36] K. Ramanathan, J. Keane, and R. Noufi, "Properties of High-Efficiency CIGS Thin-Film Solar Cells," in *Conference Record of the Thirty-first IEEE Photovoltaic Specialists Conference*, Lake Buena Vista, FL, 2005, pp. 195-198.

[37] S. Matsuda, M. Imaizumi, O. Anzawa, S. Kawakita, T. Sumita, K. Aoyama, and N. Tanioka, "Radiation Effects in Space on Solar Cells Developed for Terrestrial Use Demonstrated by MDS-1," in *Proceedings of Third World Conference on Photovoltaic Energy Conversion*, Osaka, Japan, 2003, pp. 642-645.

[38] A. Jasenek and U. Rau, "Defect Generation in Cu(In,Ga)Se$_2$ Heterojunction Solar Cells by High-Energy Electron and Proton Irradiation," *J. Appl. Phys.,* vol. 90, no. 2, pp. 650-658, Jul., 2001.

[39] F. Dimroth, C. Baur, A.W. Bett, W. Kostler, M. Meusel, and G. Strobl, "Thin 5-Junction Solar Cells with Improved Radiation Hardness," in *Conference Record of the 2006 IEEE 4th World Conference on Photovoltaic Energy Conversion,* Waikoloa, HI, 2006, pp. 1777-1780.

[40] A.F.W. Willoughby, "The Control of Radiation Resistance in Space Solar Sells," *Int. J. Electronics*, vol. 76, no. 5, pp. 865-882, 1994.

[41] C.J. Keavney, R. J. Walters, and P. J. Drevinsky, "Optimizing the Radiation Resistance of InP Solar Cells: Effect of Dopant Density and Cell Thickness," *J. Appl. Phys.*, vol. 73 (1), pp. 60-71, Jan., 1993.

[42] R.J. Walters, S. R. Messenger and H.L. Cotal, M.A. Xapos, S. J. Wojitczuk and H. B. Serreze, and G. P. Summers, "Radiation Response of Heteroepitaxial n$^+$p. InP/Si Solar Cells," *J. Appl. Phys.*, vol. 82, no. 5, pp. 2164-2175, Sept., 1997.

[43]   Y. Sun, J.M. Woodall, J.L. Freeout, and R. J. Walters, "Radiation Hard and Gravimetric Efficient Thin Film InP Solar Cells," in *Conference Record of the Twenty-Ninth IEEE Photovoltaic Specialists Conference*, New Orleans, LA, 2002, pp. 994-997.

[44]   C. Morioka, M. Imaizumi, T. Ohshima, H. Itoh, and K. Kibe, "Study on Optimum Structure of AlnGaP Top Cell Triple-Junction Space Solar Cell," *Conference Record of the 2006 IEEE 4th World Conference on Photovoltaic Energy Conversion,* Waikoloa, HI, 2006, pp. 1846-1849.

[45]   M. Yamaguchi, A. Khan, S. J. Taylor, S. J. Imaizumi, T. Hisamatsu, and S. Matsuda, "A Detailed Model to Improve the Radiation-Resistance of Si Space Solar Cells," *IEEE Trans. Electron Devices,* vol. 46, no.10, pp. 2133-2138, Oct. 1999.

[46]   J. F. Ziegler, M.D. Ziegler, and J.P. Biersack. (2006). SRIM (Version 6.02) [Computer software]. Annapolis, MD: SRIM.com. Retrieved January 23, 2007. Available: http://www.SRIM.org.

[47]   SRIM, The Stopping and Range of Ions in Matter, Instruction Manual, Version 96.xx, SRIM.com, Annapolis, MD, 1996.

[48]   J. R. Woodyard, "Investigation of Proton Radiation Resistance of CIGS Solar Cells," in *Conference Record of the Thirty-first IEEE Photovoltaic Specialists Conference*, Lake Buena Vista, FL, 2005, pp. 834-837.

[49]   A. Boden, D. Braunig, J. Klaer, F.H. Karg, B. Hosselbarth, and G. LaRoche, "Proton-Irradiation of Cu(In,Ga)Se$_2$ and CuInS$_2$ thin-film Solar Cells," in *Conference Record of theTwenty-Eighth IEEE Photovoltaic Specialists Conference*, Anchorage, AK, 2000, pp. 1038-1041.

[50]   M. Kroon, G. Oomen, and R. van der Heijden, "End-of-Life Power Predictions of Cu(In,Ga)Se$_2$ Solar Cells," in *Proceedings of Third World Conference on Photovoltaic Energy Conversion*, Osaka*,* Japan, 2003, pp. 809-812.

[51]   W. Stuckey and M. J. Meshishnek. (2003). Ground Testing of Spacecraft Materials. *Crosslink: The Aerospace Corporation Magazine of Advances in Aerospace Technology* [Online]. Available: *h*ttp://www.aero.org/publications/crosslink/summer2003/07.html

[52]   Center for Nanotechnology Education and Utilization, Pennsylvania State University, "About AMPS," July 2007, http://www.cneu.psu.edu/amps/about.html.

[53]   R. J. Walters, J. A. Warner, G. P. Summers, S. R. Messenger, J. R. Lorentzen, P. Tlomak, J. E. Grenada, and P. E. Hausgen, "Radiation Response and Annealing Characteristics of Thin Film Photovoltaics," in *Proceedings of the 19th European Photovoltaic Solar Energy Conference and Exhibition*, Paris, France, 2004.

[54]   R. J. Walters, T.L. Morton, and S. R. Messenger, NASA, "Displacement Damage Effects in Solar Cells-Mining Damage From the Micoelectronics and Photonics Test Bed Space Experiment," August, 2004, http://lws-set.gsfc.nasa.gov/Documents/R.Walters.pdf.

[55]   A. Jasenek, U. Rau, K.Weinert, H.W. Schock, and J. H. Werner, "Radiation Response of Cu(In,Ga)Se$_2$ Solar Cells," *Journal of Applied Physics*, vol. 90, no. 2, pp. 650-658, July 2001.

[56]   S. Kawakita, M. Imaizumi, M. Yamaguchi, K. Kushiya, T. Oshima, H. Ito, and S. Matsuda, "In-Situ Measurement of Degradation of Cu(In,Ga)Se$_2$ Thin Film Solar Cells During Electron and Proton Irradiations," in *Conference Record of the Twenty-Ninth IEEE Photovoltaic Specialists Conference*, New Orleans, LA, 2002, pp. 978-981.

[57]   K. Weinert, M. Schwickert, and U. Rau, "Irradiation of Cu(In,Ga)Se$_2$ Thin-Film Solar Cells with 110-, 210-, and 290-keV Protons," in *Proceedings of Third World Conference on Photovoltaic Energy Conversion*, Osaka, Japan, 2003, pp. 697-700.

[58]   D. Neamen, *Semiconductor Physics and Devices: Basic Principles*, 3rd ed. New York, NY: McGraw-Hill, 2003.

[59]   Photovoltaics CDROM, Integrative Graduate Education and Research Traineeship at the University of Deleware, "Fill Factor," March 2007, www.udel.edu/igert/pvcdrom/CELLOPER/ff.htm.